Palaeogeography, Palaeoclimatology, Palaeoecology 440 (2015) 374–394

Contents lists available at ScienceDirect

Palaeogeography, Palaeoclimatology, Palaeoecology

journal homepage: www.elsevier.com/locate/palaeo

Environmental controls on the post-Permian recovery of benthic, tropical marine ecosystems in western Palaeotethys (Aggtelek Karst, Hungary)

William J. Foster [a,b,*], Silvia Danise [a,c], Alexa Sedlacek [d], Gregory D. Price [a], Kinga Hips [e], Richard J. Twitchett [b]

[a] Plymouth University, School of Geography, Earth and Environmental Sciences, Drake Circus, Plymouth, Devon PL4 8AA, UK
[b] Natural History Museum, Department of Earth Sciences, Cromwell Road, London SW7 5BD, UK
[c] Department of Geology, University of Georgia, Athens, GA 30602-2501, USA
[d] Department of Earth Science, University of Northern Iowa, Cedar Falls, IA 50614, USA
[e] MTA-ELTE Geological, Geophysical and Space Science Research Group, Pázmány s. 1/c, 1117 Budapest, Hungary

ARTICLE INFO

Article history:
Received 13 March 2015
Received in revised form 5 September 2015
Accepted 7 September 2015
Available online 12 September 2015

Keywords:
Mass extinction
Eutrophication
Benthic recovery
Marine invertebrates
Anoxia
Early Triassic

ABSTRACT

Climate warming during the late Permian is associated with the most severe mass extinction event of the Phanerozoic, and the expansion of hypoxic and anoxic conditions in shallow shelf settings. It has been hypothesised that wave aeration provided a 'habitable zone' in the shallowest environments that allowed the survival and rapid recovery of benthic invertebrates during the Early Triassic. We test this hypothesis by studying the rock and fossil records of the Aggtelek Karst, Hungary. Nearshore settings recorded in the Bódvaszilas Sandstone Formation and units A and D of the Szin Marl Formation are characterised by taxonomically homogenous fossil assemblages of low diversity and low evenness. Ecological and taxonomic recovery in this environmental setting was hampered by persistent environmental stress. This stress is attributed to increased runoff related to climate warming during the Early Triassic that resulted in large salinity fluctuations, increased sedimentation rates and eutrophication that led to seasonal hypoxia and an environment only favourable for opportunistic taxa. In contrast, shoal and mid-ramp settings further offshore are characterised by high diversity faunas with a greater functional complexity. Prior to the late Spathian *Tirolites carniolicus* Zone, the shelly fossils and trace fossils are limited to settings aerated by wave activity, which supports the habitable zone hypothesis. In the *Tirolites carniolicus* Zone, however, the oxygen minimum zone retreats offshore and the habitable deeper shelf settings are rapidly colonised by shallow water taxa, evidenced by the highest levels of diversity and bioturbation recorded in the study. Locally, full recovery of marine ecosystems is not recorded until the Illyrian, with the establishment of a sponge reef complex.

1. Introduction

Climate warming during the late Permian, 252.28 ± 0.08 million years ago (Shen et al., 2011), is associated with Siberian Traps volcanism and the most catastrophic extinction event of the Phanerozoic (McGhee et al., 2013; Payne and Clapham, 2012). Knowledge of the post-extinction recovery of marine ecosystems is incomplete and interpretations vary depending on the temporal, spatial, ecological or taxonomic scale of analysis and the parameters used to define or quantify 'recovery'. At one extreme is the traditional view of a lengthy or delayed recovery (e.g. Hallam, 1991). This view is most evident in global-scale analyses; for example, it apparently took ca. 100 million years for family-level marine diversity to return to pre-extinction levels (Benton and Twitchett, 2003). Full recovery is typically described as occurring in the late Anisian, approximately eight million years after the late Permian mass extinction, and signalled by the return of many Lazarus taxa (Erwin and Pan, 1996), a marked increase in the diversity of bivalves (Posenato, 2008a) and other groups, reappearance of metazoan reef communities (Velledits et al., 2011), and reappearance of stenotopic hard bottom dwellers (Posenato, 2002), amongst others. There are, however, significant biases in the Early and Middle Triassic rock and fossil records, and the global Anisian dataset is skewed towards tropical, Palaeotethyan occurrences (Foster and Twitchett, 2014). This regional and latitudinal bias is likely to be impacting our understanding of global-scale post-Permian recovery, and current evidence demonstrates that recovery rates differed in different latitudes, ocean basins and depositional settings (Foster and Twitchett, 2014).

At local scales, ecosystem recovery may be tracked using a palaeoecological or functional approach (e.g. Twitchett, 2006), analogous to that used to document local recovery from episodes of environmental stress in modern marine ecosystems (e.g. Steckbauer et al.,

* Corresponding author at: Plymouth University, School of Geography, Earth and Environmental Sciences, Drake Circus, Plymouth, Devon PL4 8AA, UK.
E-mail address: w.j.foster@gmx.co.uk (W.J. Foster).

http://dx.doi.org/10.1016/j.palaeo.2015.09.004

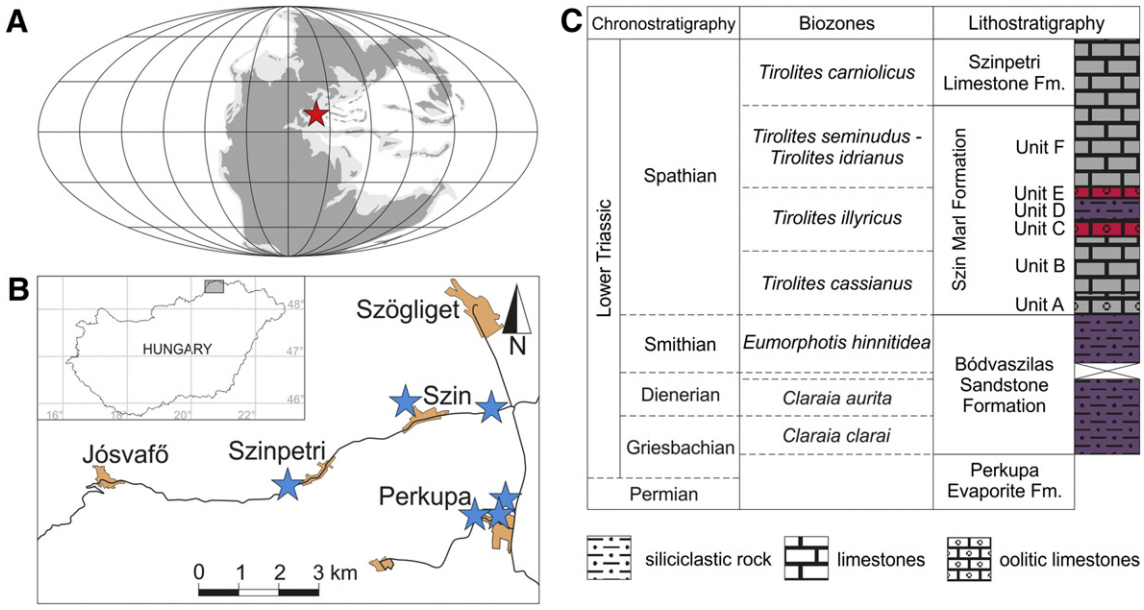

Fig. 1. Geological setting of the Aggtelek Karst. A) Palaeogeographic map of the Early Triassic after Blakey (2012) indicating approximate position of the Aggtelek Karst. B) Locality map of the study sites in the Aggtelek Karst. C) Stratigraphic subdivision of the Lower Triassic of the Aggtelek Karst (vertical subdivision is proportional to thickness; after Hips, 1996b). Biostratigraphy for the Griesbachian, Dienerian and Smithian follows the bivalve biozonation of the Werfen Formation, Dolomites (Posenato, 2008b). Biostratigraphy for the Spathian follows the ammonoid biozonation of the Werfen Formation, Dolomites, Csopak Marl Formation, Bakony, and the Muć section, Croatia (Posenato, 1992).

2011). Studies have shown that rates of post-Permian recovery varied locally. Advanced recovery had taken place in offshore seamount settings of Neotethys (Twitchett et al., 2004) and in the northwest shelf of Pangaea (Zonneveld et al., 2010) by the second conodont zone of the Triassic, within a few hundred thousand years of the extinction. Shelf locations within the palaeotropics evidently took longer to reach the same stage (Twitchett et al., 2004), although some moderate recovery has been identified locally in the late Griesbachian (Hofmann et al., 2011). The situation locally and globally was undoubtedly complex, and may have varied between habitats and taxonomic and functional groups. It has been suggested that rapid recovery was only possible in locations where benthic invertebrates were protected from environmental stresses such as marine hypoxia, and were confined to areas that were aerated by wave activity (Beatty et al., 2008; Zonneveld et al., 2010). This 'habitable zone' hypothesis may explain why local recovery was patchy and variable through the Early Triassic.

Our understanding of how marine ecosystems recovered in the aftermath of the late Permian mass extinction is therefore incomplete. The main aim of this study is to analyse the recovery of benthic invertebrate communities inhabiting a storm-influenced homoclinal ramp at

Table 1
Sedimentary facies and depositional environments for the Lower Triassic succession of the Aggtelek Karst.
After Hips (1998).

Facies	Lithology	Sedimentary structures	Depositional environment
1	Purple siltstones, very fine- to fine-grained sandstones.	Laminated siltstones and flaser bedded sandstones. Desiccation cracks, ripple marks, wrinkle marks and small domes on the siltstones.	Tidal-Flat
2	Purple siltstones, green clay, brown sandstones and grey packstones.	Laminated siltstones displaying ripples, wrinkle marks, and small ball and pillow structures (~5 cm diameter). Massive and graded sandstones.	Inner ramp, lower shoreface
3	Brown sandstones and purple siltstones.	Thick-bedded sandstones with large ball and pillow structures. Thin-bedded, graded sandstones. Hummocky and hummocky cross-stratified, fine grained sandstones. Wave rippled siltstones.	Mid-ramp, deep subtidal
4.1	Varicoloured (orange, black and yellow) oolitic grainstones.	Hummocky tops and hummocky cross-stratification. Ooids with nuclei of bioclast fragments.	Ooidal shoal and storm sheets
4.2	Red oolitic pack- and grainstones, Bedded grey wackestones and brown and purple siltstones.	Thick oolite beds with erosive bases. Bedded wackestones. Laminated siltstones.	Ooidal storm sheets
5.1	Grey fine-grained sandstones, sandy wackestones and light yellow siltstones.	Hummocky and swaley cross stratification with planar bases. Laminated siltstones.	Mid-ramp, sandy storm sheets
5.2	Green, bedded fine-grained sandstones. Green sandy limestones and siltstones.	Laminated siltstones. Large ball and pillow structures.	Mid-ramp, storm sheets
6.1	Purple and green siltstones and sandy limestones.	Laminated and bioturbated siltstones. Gutter casts on the base of limestone beds or as lenses within siltstones. Cross-laminated sandy limestone beds.	Outer ramp, distal storm layers
6.2	Grey, silty limestones, very-fine sandy limestones and grey crinoidal packstones	Laminated silty limestones. Thin-bedded sandy limestones. Crinoidal packstones. Small ball and pillow structures.	Outer ramp, distal storm layers
7	Beige, green tinted silty limestone. Green marls.	Laminated marls. Small ripples and glauconite on the thin-bedded silty limestones.	Outer ramp, low-energy
8	Light grey wackestones and dark grey packstones.	Wackestones are intensely bioturbated (ii4–5) overprinting original sedimentary structures.	Outer ramp, bioturbated

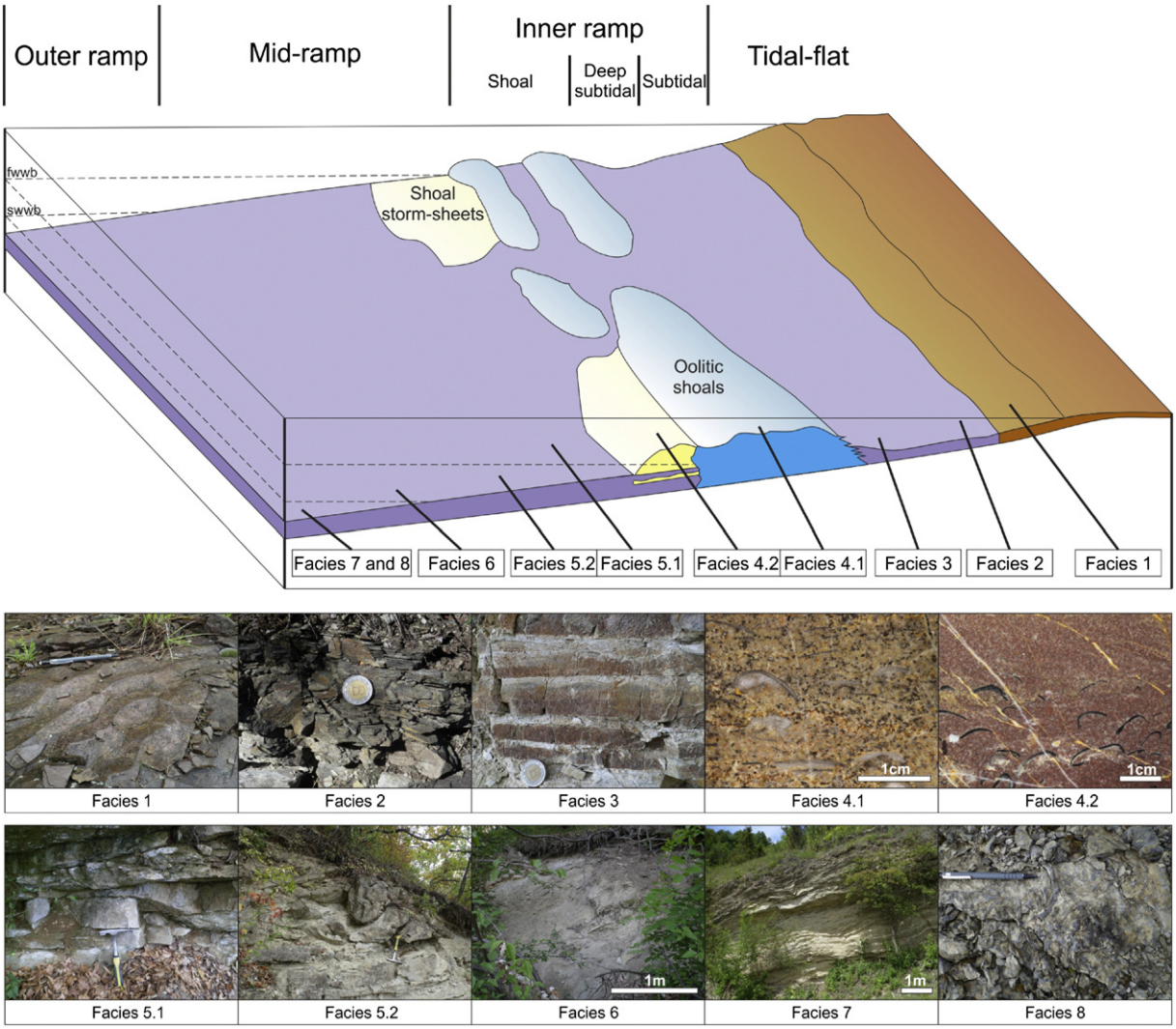

Fig. 2. Schematic model of a homoclinal ramp illustrating depositional environments and main sedimentary facies of the Lower Triassic succession of the Aggtelek Karst. Scale: coin is 10 mm, pencil is 15 cm, and hammer is 30 cm.

localities in the Aggtelek Karst of Hungary that have hitherto not been studied. In particular, we aim to assess (i) if the benthic fauna was restricted to settings aerated by wave activity, and (ii) the temporal aspects of Early Triassic recovery. These data will then be compared to other investigated localities and to a variety of palaeoenvironmental and climatic proxies.

2. Geological and stratigraphical setting

The Aggtelek Karst is a part of the South Gemer in northern Hungary which neighbours the Slovak Karst on the Hungarian-Slovakian border. During the Late Palaeozoic and Early Mesozoic it was located on the Alpine-Carpathian shelf (Csontos and Vörös, 2004; Fig. 1A). On the Hungarian side, the non-metamorphic Lower Triassic formations are known from the Silica Nappe (Kovács et al., 1989). On the Slovakian side (Slovak Karst), Lower Triassic formations are also present in the Tornaicum Nappe (Šimo and Olšavskỳ, 2007). During the Early Triassic, the depositional area of the Aggtelek Karst comprised a segment of the western Palaeotethyan shelf at an equatorial northerly latitude (Scholger et al., 2000; Kovács et al., 2011) and deposition took place on a homoclinal ramp (Hips, 1998). Detailed descriptions of the facies and ramp evolution of the Lower Triassic succession are given by Hips (1996b, 1998). This study follows Hips (1998), who recognised sixteen facies, eight of which were observed in this study (Table 1; Fig. 2; Supplementary Material), representing tidal-flat, lower shoreface, deep subtidal, shoal, mid-ramp and outer ramp depositional environments.

The Lower Triassic succession is represented by four formations: the Perkupa Evaporite, Bódvaszilas Sandstone, Szin Marl and Szinpetri Limestone. Details of their stratigraphic framework are given by Hips (1996a, 1996b). Hips (1996b) and Hips and Pelikán (2002) found that the Lower Triassic ammonoid and bivalve biozonations of the Italian Werfen Formation are applicable to the Aggtelek Karst succession (Fig. 1C), although the biostratigraphy is not well constrained and of low resolution. The entire succession is divided into five biozones: three bivalve zones and two ammonoid zones (Fig. 1C). The Perkupa Evaporite Formation was not sampled in this study, but the occurrence of *Claraia clarai* at the base of the overlying Bódvaszilas Sandstone Formation implies that both the Permian/Triassic boundary and late

Fig. 3. Logs of the Aggtelek Karst that show the facies and stratigraphic intervals of the Lower Triassic. A) Perkupa Quarry, B) Perkupa Cemetery, C) Perkupa West, D) Perkupa Vineyard, E) Szinpetri Quarry and F) Szin North. II = Ichnofabric Index (Droser and Bottjer, 1986). Grain size scale: C = clay, S = siltstone, VF = very fine sand, F = fine sand, M = medium sand, m = mudstone, w = wackestone, p = packstone, g = grainstone.

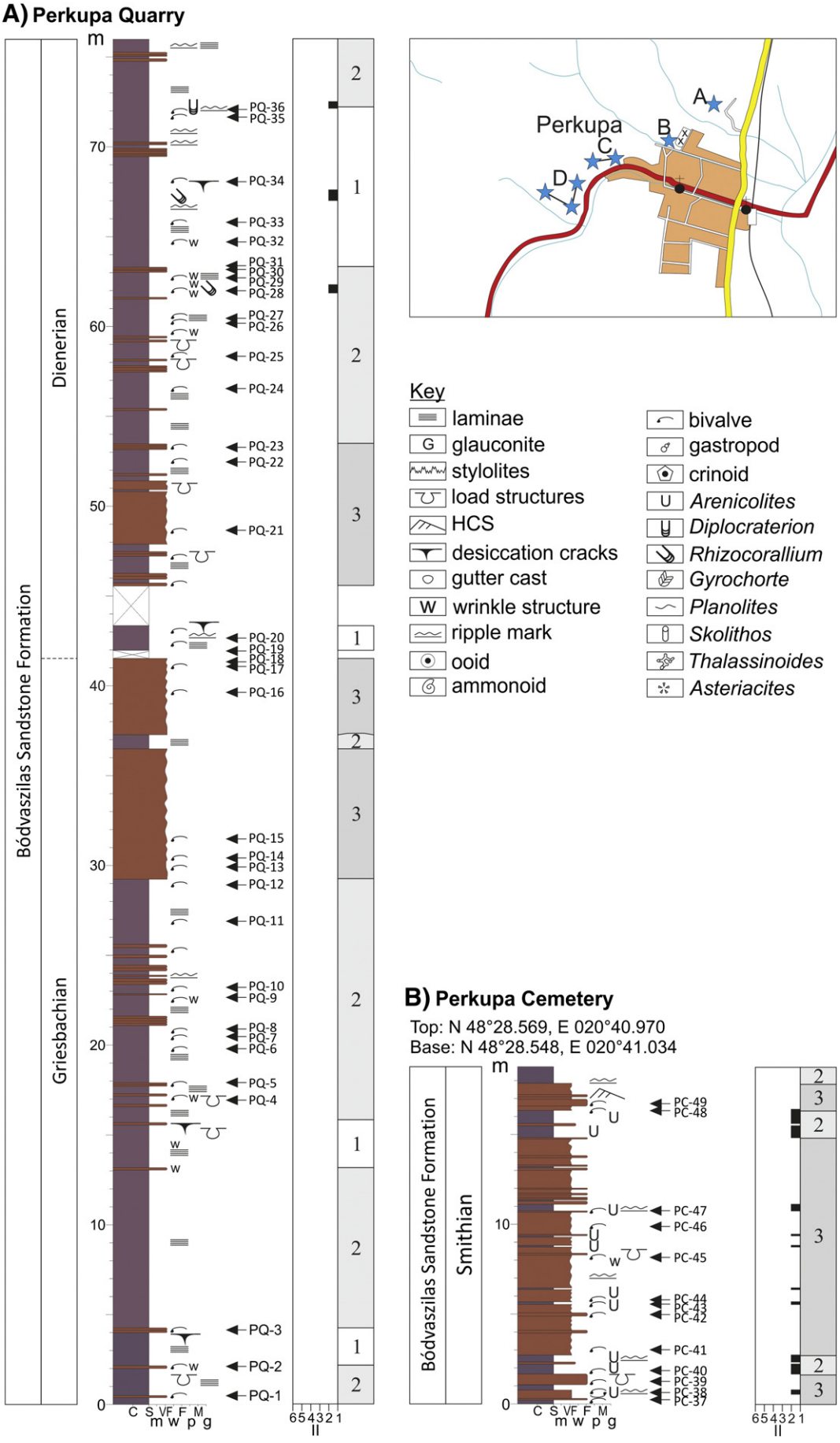
A) Perkupa Quarry
Bódvaszilas Sandstone Formation
Dienerian
Griesbachian
m
PQ-36
PQ-35
PQ-34
PQ-33
PQ-32
PQ-31
PQ-30
PQ-29
PQ-28
PQ-27
PQ-26
PQ-25
PQ-24
PQ-23
PQ-22
PQ-21
PQ-20
PQ-19
PQ-18
PQ-17
PQ-16
PQ-15
PQ-14
PQ-13
PQ-12
PQ-11
PQ-10
PQ-9
PQ-8
PQ-7
PQ-6
PQ-5
PQ-4
PQ-3
PQ-2
PQ-1
C S VF F M
m w p g
65432 1
II
Perkupa
A
B
C
D
Key
laminae
glauconite
stylolites
load structures
HCS
desiccation cracks
gutter cast
wrinkle structure
ripple mark
ooid
ammonoid
bivalve
gastropod
crinoid
Arenicolites
Diplocraterion
Rhizocorallium
Gyrochorte
Planolites
Skolithos
Thalassinoides
Asteriacites
B) Perkupa Cemetery
Top: N 48°28.569, E 020°40.970
Base: N 48°28.548, E 020°41.034
Bódvaszilas Sandstone Formation
Smithian
PC-49
PC-48
PC-47
PC-46
PC-45
PC-44
PC-43
PC-42
PC-41
PC-40
PC-39
PC-38
PC-37

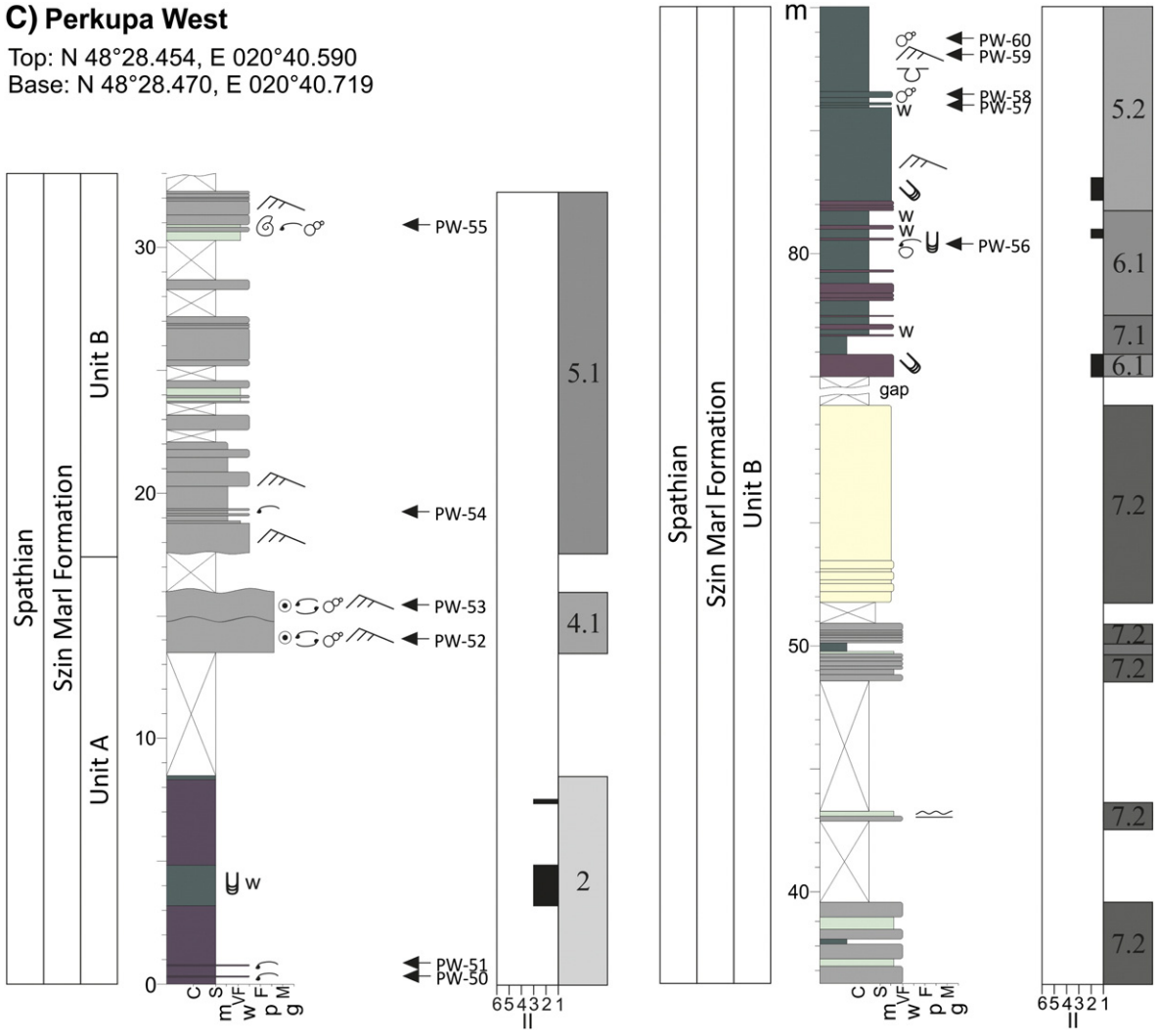

Fig. 3 (*continued*).

Permian extinction occurred during deposition of the Perkupa Evaporite Formation (Hips, 1996b). The Bódvaszilas Sandstone Formation spans the late Griesbachian *C. clarai* Zone, the Dienerian *C. aurita* Zone and the Smithian, *Eumorphotis hinnitidea* Zone (Fig. 1C). Hips (1996b) identified the Szin Marl and Szinpetri Limestone formations as Spathian based on the occurrence of the ammonoids *Tirolites cassianus* and *T. carniolicus*. Furthermore, *T. carniolicus* occurs in the lower part of the Szinpetri Limestone Formation and indicates a late Spathian age (Posenato, 1992). Novel strontium isotope data support an upper Spathian age for the Szinpetri Limestone ($^{87}Sr/^{86}Sr = 0.7081$), although data from the underlying Szin Marl Formation are more radiogenic than reported for the Spathian (Korte et al., 2003) and consistent with alteration to more radiogenic values during diagenesis (Appendix A). The Lower/Middle Triassic boundary is tentatively placed at the base of the overlying Gutenstein Formation, but there is a lack of age-diagnostic fossils (Hips, 2007).

3. Methods

3.1. Sample collection

Six sections were investigated near the villages of Perkupa, Szin and Szinpetri (Fig. 1B). Sedimentary logs were produced in the field in June, July and September 2012 and May 2013 (Fig. 3), using the formation and unit/member definitions of Hips (1996b). Lithologies, sedimentary structures, trace fossils and ichnofabric index (ii; Droser and Bottjer, 1986) were described for each measured bed. Fossiliferous beds were quantitatively sampled for macrofossils. Laminated beds were sampled by collecting 2 kg samples of bulk rock, which were then split parallel to bedding in the field to reveal the fauna. All fossils were identified and counted in the field, with reference samples taken for laboratory preparation and further taxonomic identification.

Consolidated beds that could not be split easily in the field were hand-sampled by collecting blocks at least 5 cm across and 5 cm thick. If the bed was thicker than one metre, a sample was collected every metre. The difficulty of removing and identifying small shells from consolidated samples is a significant obstacle to detailed taxonomic study of those fossils not easily classified from thin sections (Payne et al., 2006a). As an improvement, in this study the consolidated samples were cut into 5 × 5 cm slabs, which were polished on one side and then analysed using an equal area approach (cf. Jacobsen et al., 2011). This polished slab technique is simpler, faster and requires less equipment than standard thin-sectioning, but its key advantage is that the polished slabs are larger and thus are more likely to allow the identification of enough bioclasts for statistical palaeoecological analysis. Polished slabs enable relative abundances to be assessed across a greater size- and taxonomic range, and the inclusion of invertebrates that are too small to be counted using conventional methods, such as microconchids which commonly

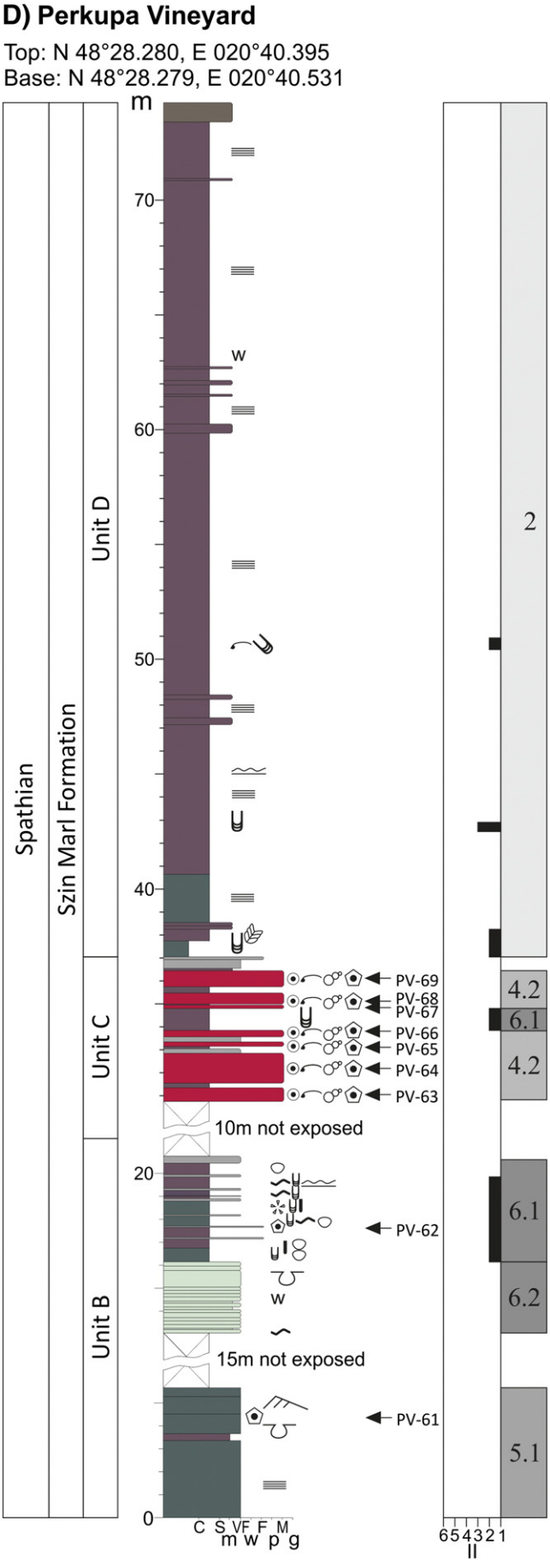

Fig. 3 (*continued*).

dominate some Lower Triassic beds (e.g. Zatoń et al., 2013). It also facilitates standardised sampling by allowing the investigator to search the same area of rock in each sample.

One representative individual of each species that was identified from bedding plane surfaces was sliced vertically. The distinguishing characteristics of each taxon in vertical section were then documented (see Supplementary Materials), and used to identify specimens in the polished slabs. All identifiable fossils in the polished slabs were identified to the lowest taxonomic level to which they could be confidently assigned (Supplementary Material). Taxonomic resolution varied between fossil groups, ranging from species- to phylum-level. Bioclasts were counted by placing a 5 × 5 cm acetate sheet over the polished surface of each sample. This sheet was divided into one hundred 5 mm square divisions, which aided counting (i.e. to not count the same clast twice). All the bioclasts within the 5 × 5 cm quadrat were identified to measure taxonomic richness and tallied to obtain abundance data.

3.2. Palaeoecological analysis

The palaeoecological analysis was limited to benthic marine invertebrates, thus excluding ammonoids, conodonts, algae and foraminifera. Using raw, disarticulated bioclast counts in palaeoecological analyses is complicated by differences in skeletal element composition between different taxonomic groups, e.g. bivalves comprise two valves whereas crinoids may disarticulate into thousands of ossicles. The common approach followed in this study is to use estimates of minimum numbers of individuals (MNI) for all analyses. For all taxa, a complete, fully articulated specimen represents a single individual. For disarticulated bivalves, two opposing valves of a similar size (within 1 mm) were counted as one individual, and each valve of unequal size as an individual. For disarticulated brachiopods and ostracods, two opposing valves were counted as one individual. Where size measurements were not possible and valves could not be identified, the number of individuals was equal to the total number of valves divided by two. For gastropods, the number of individuals was equated to the number of individual apices. Those gastropods that were oriented transversely to the polished slab, and thus unidentifiable, were excluded. For microconchids and scaphopods, each bioclast was considered to represent a separate individual. As echinoderms can potentially disarticulate into hundreds or thousands of ossicles (e.g. Schubert et al., 1992; Twitchett et al., 2005), estimating their abundance is problematic. Schubert et al. (1992) calculated that approximately 1500 ossicles represent a single *Holocrinus* individual, and this value is used herein to calculate crinoid MNI. For ophiuroids, approximately thirty ossicles were counted from each arm of Early Triassic specimens from the Werfen Formation, Italy, (Hofmann et al., 2015) and Changhsing Formation, China, (Chen et al., 2004), and so an estimate of 150 ossicles per individual is used herein to calculate MNI.

Twenty individuals per sample is the minimum required to begin to capture community signals for ecological analysis (Webb and Leighton, 2011; Patzkowsky and Holland, 2012), and so samples with MNI < 20 were excluded from further analysis. The analysis was carried out at the lowest taxonomic level possible. Since multiple methods were used, i.e. mechanical disaggregation and polished slabs, the analysis was carried out using the taxonomic resolution recognised by the polished slab technique; e.g., because *Unionites* was only identified to genus-level in polished slabs, despite being identifiable to species-level using mechanical disaggregation, the analysis was carried out at genus-level for *Unionites*. This allowed the different collection methods to be analysed synchronously.

3.3. Functional diversity

Each taxon was assigned to a bin in the ecospace model of Bambach et al. (2007) based on its tiering, motility and feeding, using data from

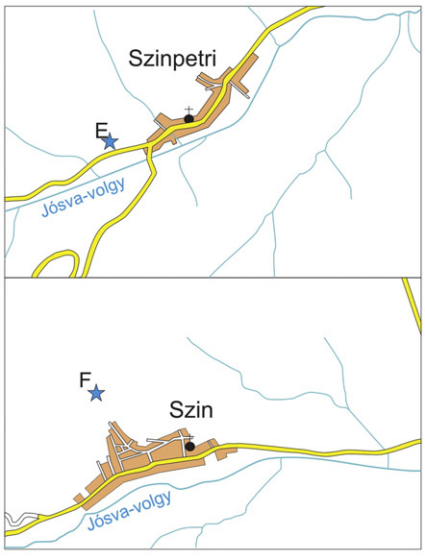

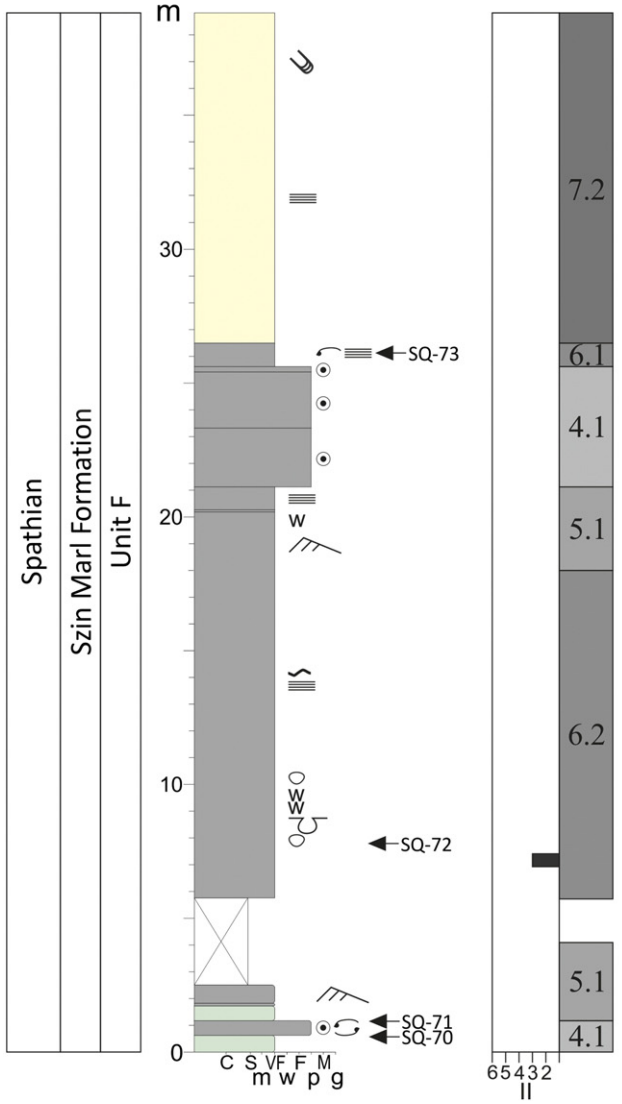

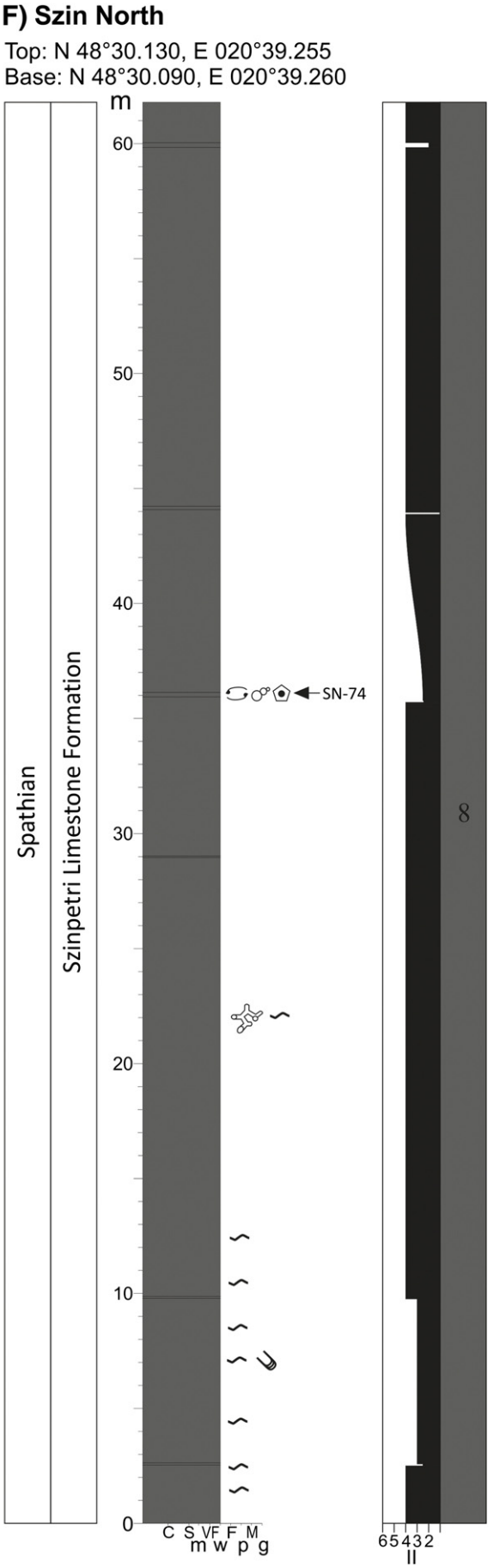

Fig. 3 (*continued*).

extant relatives, previous publications and functional morphology. As some marine animals utilise different modes of life through ontogeny, each taxon was assigned a mode of life applicable to the adult life stages (following Bambach et al., 2007). Each mode of life was assigned to the highest taxonomic resolution for each taxon, i.e. genus- to order-level, and follows Bush et al. (2007). For example, although scaphopods feed on foraminifera Bush et al. (2007) considered them to be miners, not predators, because foraminifera are 'small, buried, food particles'. In cases where interpretation of a taxon's tiering, motility and feeding is problematic, the most up-to-date or most widely accepted analysis was followed.

3.4. Analytical methods

For each sample, alpha diversity was measured using taxonomic richness (S) and Simpson index of diversity (1-λ). Diversity metrics are not independent of abundance where S provides information on the rare tail of the taxon abundance distribution and Simpson's D reflects the abundant end of the distribution. These were used in concert to understand how abundance contributes to changes in alpha diversity in a broad sense. Species Richness and Simpson's Diversity were computed in PAST (Hammer et al., 2001). Whereas Simpson's D is biased by sample size and richness (Olszewski, 2004), Hurlbert's PIE is not biased and uses Simpson D to calculate the probability of an interspecific encounter (Olszewski, 2004). These diversity indices are useful in estimating diversity, but are not measures of diversity (Jost, 2006). Bias-corrected Simpson D values (Δ) were therefore converted into effective diversities following Jost (2006).

For multivariate elaboration, samples that only contain species found in no other sample were removed because such samples would have zero similarity to any other sample and would plot randomly in an ordination and as an outlier in a cluster analysis. Relative, rather than absolute, abundances were used as preservation varies between samples (Clarke and Warwick, 2001) and multiple methods were used. Most of the samples are dominated by a few taxa, and so the relative abundance data were square-root transformed to de-emphasise the influence of the most dominant taxon (Clarke and Warwick, 2001).

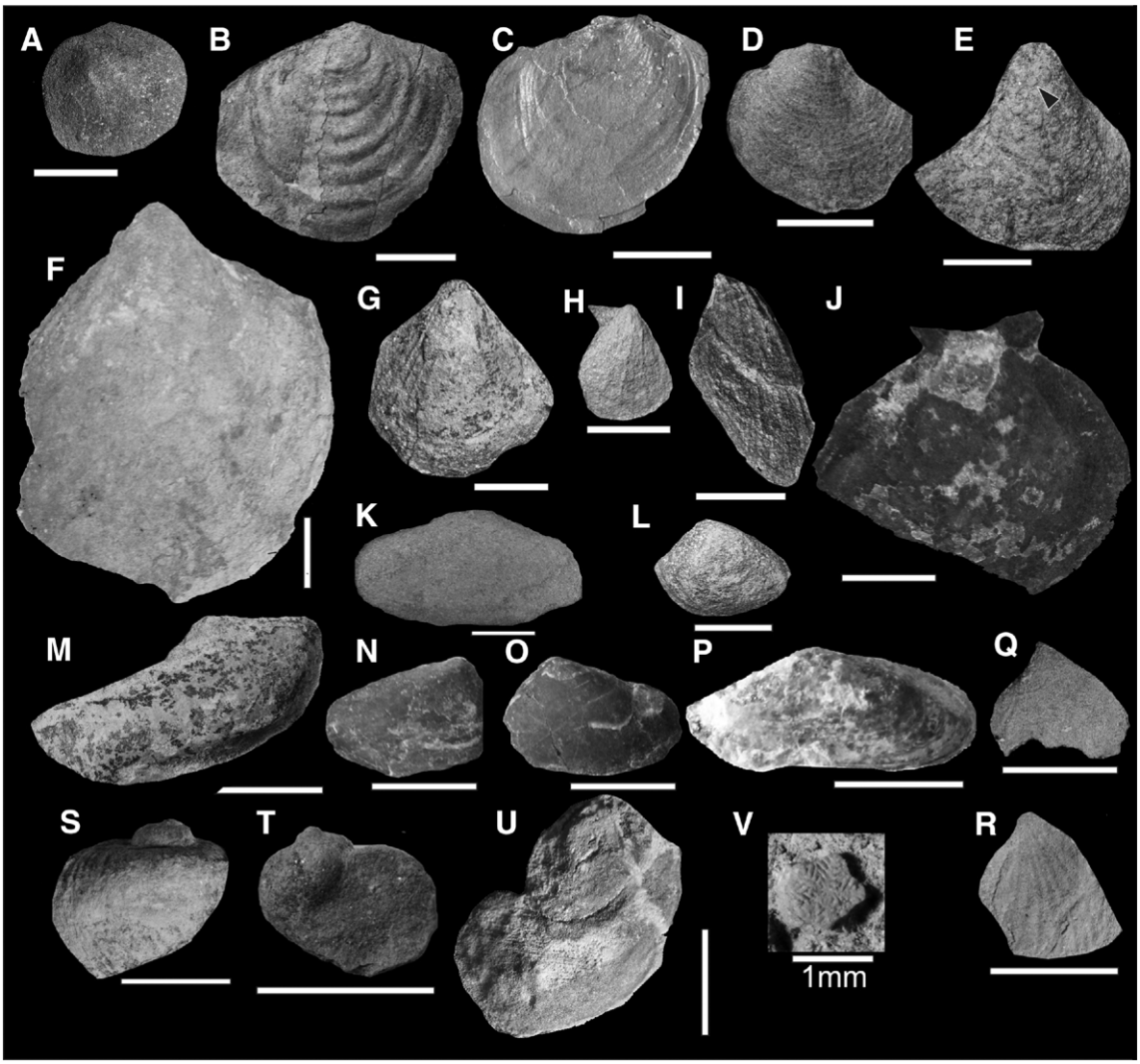

Fig. 4. Fossil invertebrates from the Lower Triassic of the Aggtelek Karst. A) *Claraia* cf. *wangi-griesbachi*, Perkupa Quarry, 0.5 m above base of section. B) *C. clarai*, Perkupa Quarry, 41 m. C) *C. clarai*, Perkupa Quarry 4 m. D) *C. aurita*, Perkupa Quarry, 56.5 m. E) *C. aurita* encrusted with microconchids (black arrow), Perkupa Quarry, 60 m. F) *Eumorphotis* cf. *kittli*, Szinpetri Quarry 26 m. G) *E. multiformis*, Perkupa Cemetery, 8 m. H) *E. multiformis*, Perkupa Cemetery 10 m. I) *E. venetiana*, Perkupa Cemetery, 10 m. J) *Scythentolium* sp., Perkupa Vineyard, 32 m. K) cf. *Unionites canalensis*, Perkupa Quarry, 66 m. L) cf. *U. fassaensis*, Perkupa Cemetery, 5.6 m. M) *Bakevellia* cf. *incurvata*, Perkupa West, 0.5 m. N) *Neoschizodus ovatus*, Perkupa Vineyard, 32 m. O) *N. ovatus*, Perkupa Vineyard 32 m. P) cf. *Pholadomya* sp., Perkupa Vineyard, 32 m. Q, R) *Costatoria costata*, Szinpetri Quarry, 26 m. S,T) *Natiria costata*, Perkupa West, 86 m. U) *Werfenella rectecostata*, Perkupa West, 31 m. V) *Holocrinus* ossicle, Perkupa Vineyard 17 m. Scale bar = 10 mm except V.

Hierarchical agglomerative clustering (cluster analysis), using an unweighted pair-group average cluster model (Clarke and Warwick, 2001), was applied to recognise those species that tend to co-occur in samples and to group together samples of similar taxonomic composition using the Bray-Curtis similarity matrix. The similarity profile test (SIMPROF) was applied to determine significant differences between the clusters (Clarke and Warwick, 2001). Here, 999 permutations were applied to calculate a mean similarity profile, 999 simulated profiles were generated, and the chosen significance level was 0.05. The resulting clusters of samples were analysed through a similarity percentages routine (SIMPER) to determine which species were responsible for the greatest similarity within groups, i.e. the trophic nucleus (Clarke, 1993). This method enabled the identification of groups of samples that contain a similar suite of taxa in similar proportions (i.e. "biofacies" sensu Ludvigsen et al., 1986), and also to identify their characteristic species.

Non-metric multidimensional scaling (nMDS) was then applied to visualise trends and groupings of the samples. Shepard diagrams were produced for the ordinations to investigate the stress of the plot (Clarke and Warwick, 2001). Stress measures the departure of points from the best-fitting, increasing regression line. Thus, when rank order relationships are exactly preserved the stress is zero (Clarke and Warwick, 2001). Stress, therefore, indicates the quality of the nMDS plot with values of <0.05 showing an excellent representation of the data; <0.1 good representation; <0.2 acceptable representation for 2D plots only and >0.3 unsatisfactory representation (Clarke and Warwick, 2001).

A permutational ANOVA and MANOVA (PERMANOVA) were used to compare the benthic assemblages between the different facies, sub-

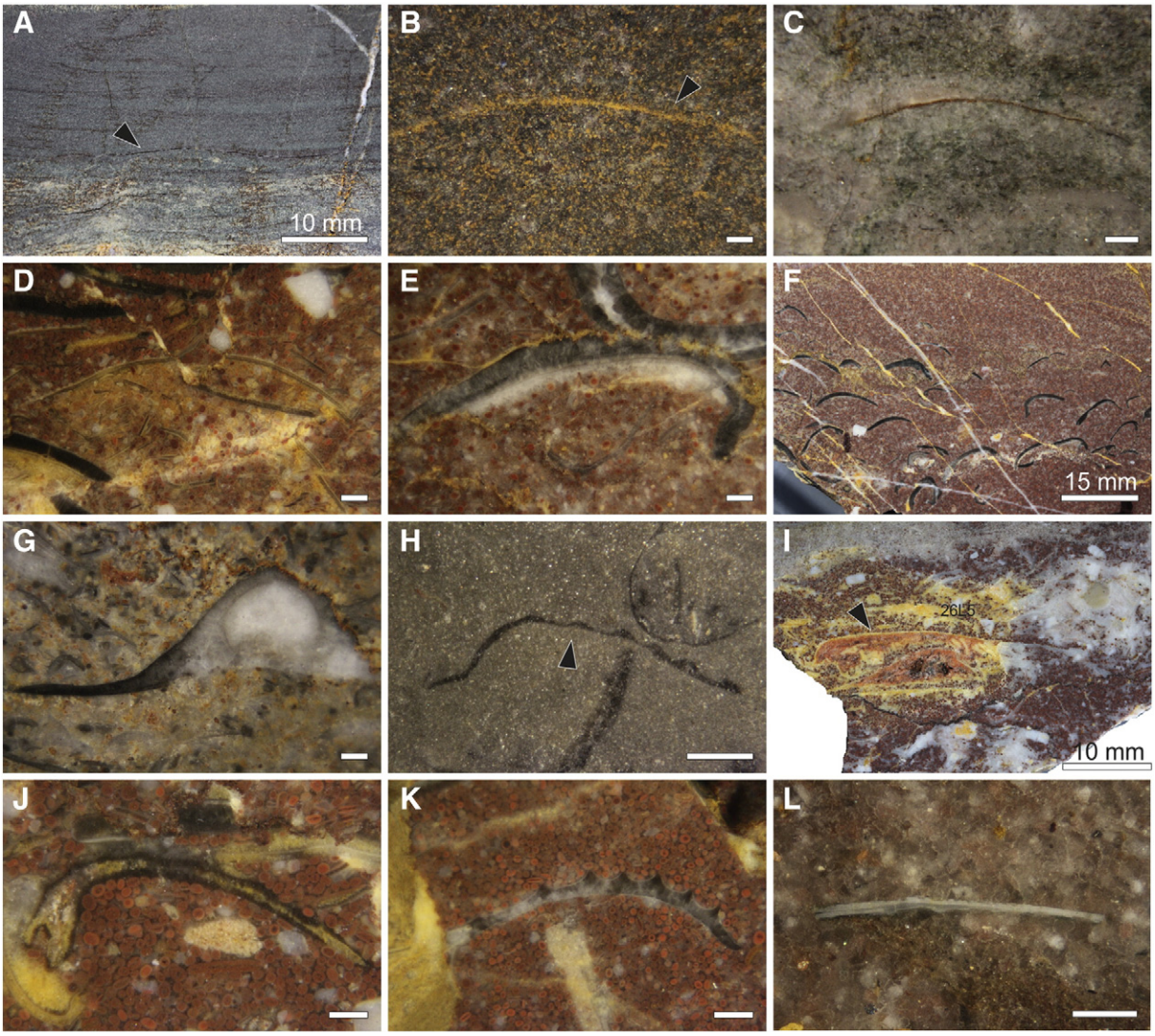

Fig. 5. Polished slabs displaying the fauna and the problematicum recognised from the Lower Triassic of the Aggtelek Karst. All specimens are wetted with water. A) *Claraia clarai*, Bódvaszilas Sandstone Formation, Perkupa Quarry section, B) *Claraia aurita*, Bódvaszilas Sandstone Formation, Perkupa Quarry section, C) cf. *Unionites*, Szin Marl Formation, Unit B, Perkupa West section, gastro scree, D) *Eumorphotis*, Szin Marl Formation, Unit C, Perkupa Vineyard, E) *Neoschizodus ovatus*, Szin Marl Formation, Unit C, Perkupa Vineyard, F) *Neoschizodus ovatus*, Szin Marl Formation, Unit C, Perkupa Vineyard, G) *Bakevellia* cf. *incurvata*, Szin Marl Formation, Unit A, Perkupa West, H) *Bakevellia* with costae, Szinpetri Limestone, Szin North, I) *Scythentolium* sp., Szin Marl Formation, Unit C, Perkupa Vineyard, J) cf. *Pholadomya* sp., Szin Marl Formation, Unit C, Perkupa Vineyard, K) *Costatoria costata*, Szin Marl Formation, Unit C, Perkupa Vineyard, L) *Lingularia* sp., Bódvaszilas Sandstone Formation, Perkupa Cemetery. M) Dentaliidae sp., Szin Marl Formation, Unit C, Perkupa Vineyard, N) *Natiria costata*, Szin Marl Formation, Unit B, Perkupa West, O) Gastropod Indet. A., Szin Marl Formation, Unit C, Perkupa Vineyard, P) *Coelostylina werfensis*, Szin Marl Formation, Unit C, Perkupa Vineyard, Q) *Coelostylina werfensis*, Szin Marl Formation, Unit F, Szinpetri Quarry, R) transverse section of a gastropod, Szin Marl Formation, Unit F, Szinpetri Quarry, S) Ophiuroid ossicle, Szinpetri Limestone, Szin North section, T) *Holocrinus* sp., Szin Marl Formation, Unit C, Perkupa Vineyard, U) *Holocrinus* sp., Szin Marl Formation, Unit B, Perkupa Vineyard, X) *Microconchus*, Bódvaszilas Sandstone Formation, Perkupa Cemetery, Y) Microconchid, Bódvaszilas Sandstone Formation, Perkupa Quarry, Z) Problematicum (cf. Porifera), Szinpetri Limestone, Szin North, Scale bar = 1 mm, except A, F and I.

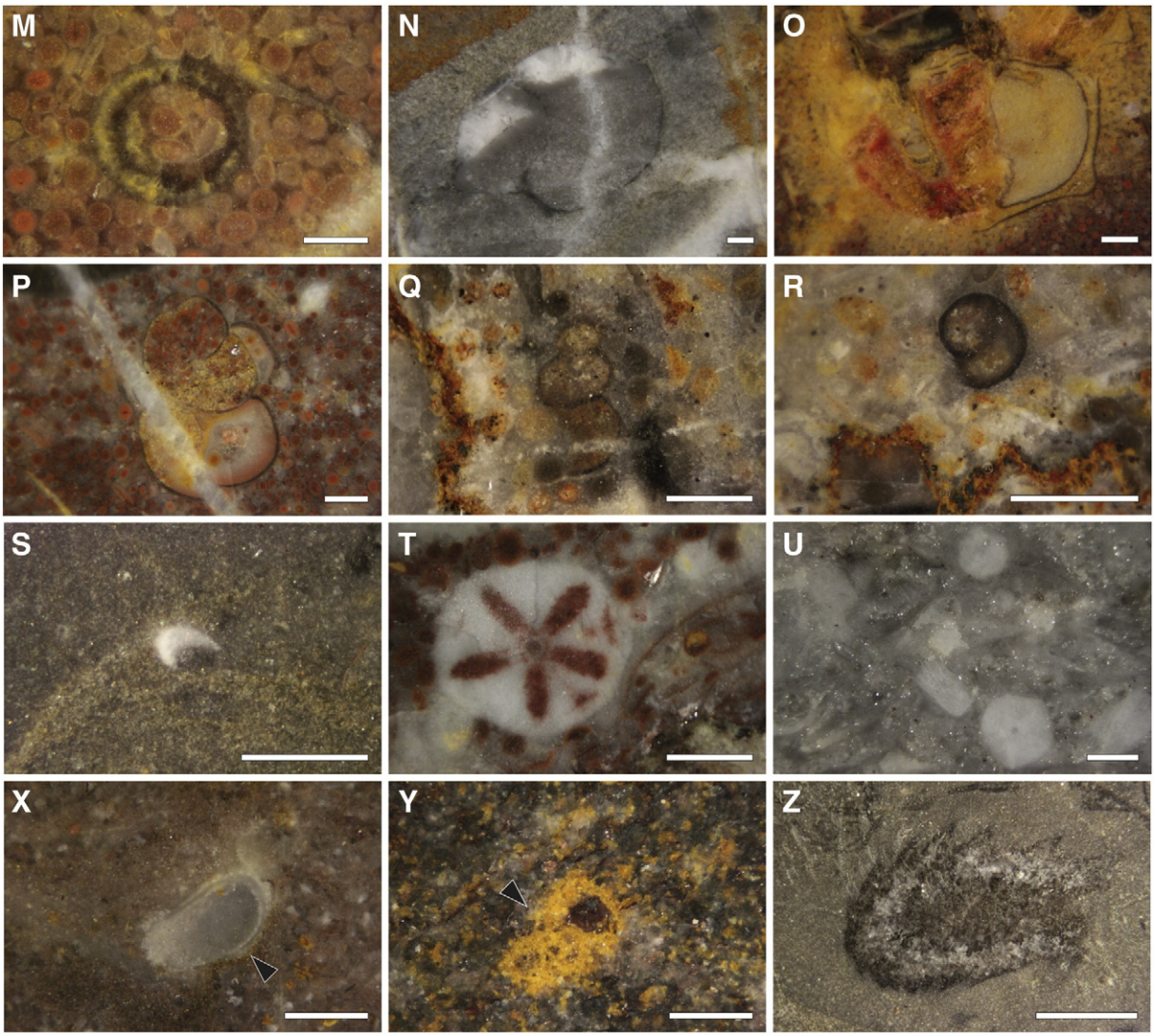

Fig. 5 (*continued*).

stages, lithologies, formations and methods (Anderson, 2001; Anderson et al., 2008). In some situations there are not enough possible unique permutations to get a reasonable test (Anderson, 2001), and so Monte Carlo P-values were also calculated. When multiple variables, e.g. formation, stage, method, facies or lithology, showed significant differences, they were then subject to pair-wise comparisons. This was done by performing a (two-tailed) *t*-test. Significance was taken at the 0.05 level. A permutational test of homogeneity of dispersions (PERMDISP) was used for testing of multivariate dispersions on the basis of a resemblance measure. This is useful because two samples may have a similar centroid in multi-dimensional space and so PERMDISP investigates if they have significantly different dispersions.

Cluster, ordination and PERMANOVA analyses were performed with the software PRIMER 6.1.15 & PERMANOVA 1.0.5.

4. Palaeoecological results

4.1. Alpha diversity

In the Aggtelek Karst, 26 species from 16 genera and one problematicum were identified from 82 Lower Triassic samples and 5,458 specimens (Figs. 4–5; Table 2). Recorded taxa include bivalves, gastropods, microconchids, crinoids, ophiuroids, brachiopods and scaphopods. Microgastropod packstones and grainstones that are common in other Lower Triassic strata (e.g. Fraiser and Bottjer, 2004) were not recorded in the Aggtelek Karst. The MNI per sample ranges from 1 to 163, and 45 samples have a large enough abundance (>20 MNI) for quantitative analysis (Supplementary Materials).

The alpha diversity indices record changes along a temporal and environmental gradient: the lowest values are recorded in the siliciclastic inner and mid-ramp settings of the Bódvaszilas Sandstone ($S = 2$–5; $\Delta = 1.1$–3.9) and Szin Marl ($S = 4$; $\Delta = 2.7$) formations, and the highest in the carbonate oolitic shoal to mid-ramp settings of the Szin Marl Formation ($S = 1$–7; $\Delta = 1$–3.7) and the outer ramp setting of the Szinpetri Limestone ($S = 11$; $\Delta = 7.4$). Significant differences between the formations, sub-stages, and lithologies (Fig. 6) are due to a greater number of facies sampled in the Szin Marl Formation compared with the Bódvaszilas Sandstone Formation. There are no significant changes in Simpson Diversity, however (Fig. 6), which suggests that the significant differences in species richness are due to changes in the rare taxa.

Within the Szin Marl Formation, species richness is significantly higher in the oolitic shoal facies association than in other facies, but Simpson Diversity is not significantly different between the different facies (Fig. 6). Therefore, the higher diversity in oolitic shoal facies is driven by a greater number of rare taxa. Benthic fauna, excluding rare crinoid ossicles, were not recorded in the outer ramp environment until unit F of the Szin Marl Formation. Only two samples were collected from outer ramp facies, and the one from the Szinpetri Limestone

Table 2
List of all recorded taxa and their mode of life. Modes of life after Foster and Twitchett (2014). T = tiering, M = motility, F = feeding. Tiering: 2 = erect, 3 = epifaunal, 4 = semi-infaunal, 5 = shallow infaunal. Motility: 2 = slow, 4 = facultative, attached, 3 = facultative, unattached, 5 = unattached, 6 = attached. Feeding: 1 = suspension feeding, 2 = surface deposit feeding, 3 = miner, 4 = grazer, 5 = predator.

Species	Group	Mode of life			Taxonomic identification after
		T	M	F	
Bakevellia with costae	Bivalve	4	4	1	Neri and Posenato (1985)
Bakevellia cf. *incurvata*	Bivalve	4	4	1	Kolar-Jurkovšek et al. (2013)
Claraia aurita	Bivalve	3	4	1	Nakazawa (1977)
Claraia clarai	Bivalve	3	4	1	Nakazawa (1977)
Claraia sp.	Bivalve	3	4	1	
Claraia cf. *wangi-griesbachi*	Bivalve	3	4	1	Broglio Loriga et al. (1983)
Costatoria costata	Bivalve	5	3	1	Broglio Loriga and Posenato (1986)
Eumorphotis hinnitidea	Bivalve	3	6	1	Broglio Loriga and Mirabella (1986)
Eumorphotis cf. *kittli*	Bivalve	3	6	1	Broglio Loriga and Mirabella (1986)
Eumorphotis multiformis	Bivalve	3	6	1	Broglio Loriga and Mirabella (1986)
Eumorphotis cf. *venetiana*	Bivalve	3	6	1	Broglio Loriga and Mirabella (1986)
Neoschizodus laevigatus	Bivalve	5	3	1	Neri and Posenato (1985)
Neoschizodus ovatus	Bivalve	5	3	1	Neri and Posenato (1985)
cf. *Pholadomya* sp.	Bivalve	5	3	1	Cox et al. (1969)
Scythentolium sp.	Bivalve	3	5	1	Neri and Posenato (1985)
cf. *Unionites canalensis*	Bivalve	5	3	1	Neri and Posenato (1985)
cf. *Unionites fassaensis*	Bivalve	5	3	1	Neri and Posenato (1985))
Gastropod Indet sp.	Gastropod	3	3	1	
Coelostylina werfensis	Gastropod	3	3	1	Nützel and Schulbert (2005)
Natiria costata	Gastropod	3	2	4	Neri and Posenato (1985)
Werfenella rectecostata	Gastropod	3	2	4	Nützel (2005)
Dentaliidae sp.	Scaphopod	4	3	3	Yochelson (2011)
Lingularia	Brachiopod	5	4	1	Posenato et al. (2014)
Holocrinus	Crinoid	2	4	1	Kashiyama and Oji (2004)
Ophiuroidea	Ophiuroid	3	2	2/5	Glazek and Radwański (1968)
Microconchus	Microconchida	3	6	1	Zatoń et al. (2013)

Formation shows the greatest alpha diversity values recorded in this study ($S = 11$; $\Delta = 7.4$).

Eleven modes of life were identified from the Aggtelek Karst (Table 2). Changes in functional diversity vary along temporal and environmental gradients: the siliciclastic inner ramp and deep subtidal settings of the Bódvaszilas Sandstone and Szin Marl formations recorded lower alpha diversity than the carbonate shoal and mid-ramp settings of the Szin Marl and outer ramp of the Szinpetri Limestone formations (Fig. 7). The Kruskal-Wallis test shows that these differences are significant, except differences in the Simpson Diversity of samples from different facies (Fig. 7). This shows that the increase in functional diversity in shoal and mid-ramp settings is driven by the increase in rare modes of life, e.g. semi-infaunal slow-moving miners.

4.2. Changes in taxonomic composition

The cluster analysis shows that two broad sample clusters are distinguished at a similarity of around 40% (Fig. 8). The first comprises samples from the Bódvaszilas Sandstone Formation and one from the outer ramp facies of the Szin Marl Formation, and is characterised by the dominance of the bivalve *Unionites* and the absence of gastropods. The second comprises samples from the Spathian Szin Marl and Szinpetri Limestone formations (Fig. 8) and is characterised by samples dominated by the bivalve *Neoschizodus ovatus* or the gastropod *Natiria costata*. The SIMPROF test applied to the cluster analysis recognised five statistically distinct groups (A-E; Fig. 8) that, together with the SIMPER analysis, enabled the identification of the trophic nucleus within each group of samples and the definition of five biofacies (Fig. 8; Supplementary Material).

The main axis of the ordination (nMDS1) mostly reflects temporal changes through the studied site, with Griesbachian samples on the left side of the diagram, through to Spathian samples on the right (Fig. 9). The stress value for the nMDS ordination is 0.07, which gives confidence that the two-dimensional plot is an accurate representation of the sample relationships (Clarke and Gorley, 2006). Induan samples overlap, indicating homogeneity, and most Smithian samples group close to the Induan samples on the nMDS plot (Fig. 9A). The distinction between the Induan and Smithian samples is due to limited taxonomic turnover (i.e. from *Claraia* in the Induan to *Eumorphotis* in the Smithian). This is supported by the pairwise PERMANOVA and PERMDISP results that only show significant differences in the Spathian (Fig. 9A; Supplementary Material).

The increased heterogeneity (i.e. sample dispersal) in the Spathian is mainly due to greater facies variation (Fig. 9). The low dispersion of samples within individual facies, excluding the deep subtidal facies, indicates within-lithofacies homogeneity. The PERMDISP results also record no significant difference in the dispersion of samples within the different facies ($p = 0.38$). The PERMANOVA shows no significant interaction in the effects of sub-stage and facies on the variability in these assemblages ($p = 0.61$), due to a low number of facies associations recognised in the Bódvaszilas Sandstone Formation.

The only facies that was recognised and quantitatively sampled in both the Bódvaszilas Sandstone and Szin Marl formations is the deep subtidal facies. The Szin Marl Formation sample is significantly distinct from the other pre-Spathian samples and is characterised by a very different fauna, i.e. *Bakevellia* not *Unionites*. The pre-Spathian samples are from siliciclastic rocks, however, whereas the Spathian samples are from carbonate. This suggests that even though there is a significant change in the deep-subtidal benthic communities between the pre-Spathian and Spathian, these differences may be due to lithological change.

Temporal changes within the Spathian can also be recognised. The outer ramp depositional environment of the Szin Marl Formation contains a less diverse and compositionally different benthos compared to that of the Szinpetri Limestone Formation (Fig. 9). The Szin Marl outer ramp sample clusters within the *Unionites-Eumorphotis* biofacies (Fig. 9c) and shows greater similarity to samples from the Bódvaszilas Sandstone Formation. The younger Szinpetri Limestone outer ramp sample, however, shows a greater resemblance to the Szin Marl mid-ramp and oolitic shoal environments. This implies that the fauna that occupied shallower environments during deposition of the Szin Marl Formation expanded into outer ramp environments during deposition of the Szinpetri Limestone Formation in the late Spathian.

4.3. Changes in ecological composition

The cluster analysis shows two major groups, one characterised by infaunal, facultatively motile, unattached, suspension feeders and the other by epifaunal, slow-moving, grazers (Fig. 10). This main division is due to major differences in facies preference: the infaunal bivalves of Group 1 occur in all the facies except the mid-ramp, which is exclusively dominated by slow-moving grazers. The SIMPROF test recognises 7 significantly different 'ecofacies' (Fig. 10; Supplementary Materials).

The stress value for the nMDS ordination is 0.05, which gives confidence that the two-dimensional plot is an accurate representation of the sample relationships (Clarke and Gorley, 2006). The two major groupings recognised in the cluster analysis are present in the nMDS plot (Fig. 11A). No strong temporal trend is recognised, although the Griesbachian, Dienerian and Smithian samples overlap in the nMDS plot, whereas the Spathian samples, which are more diverse with a

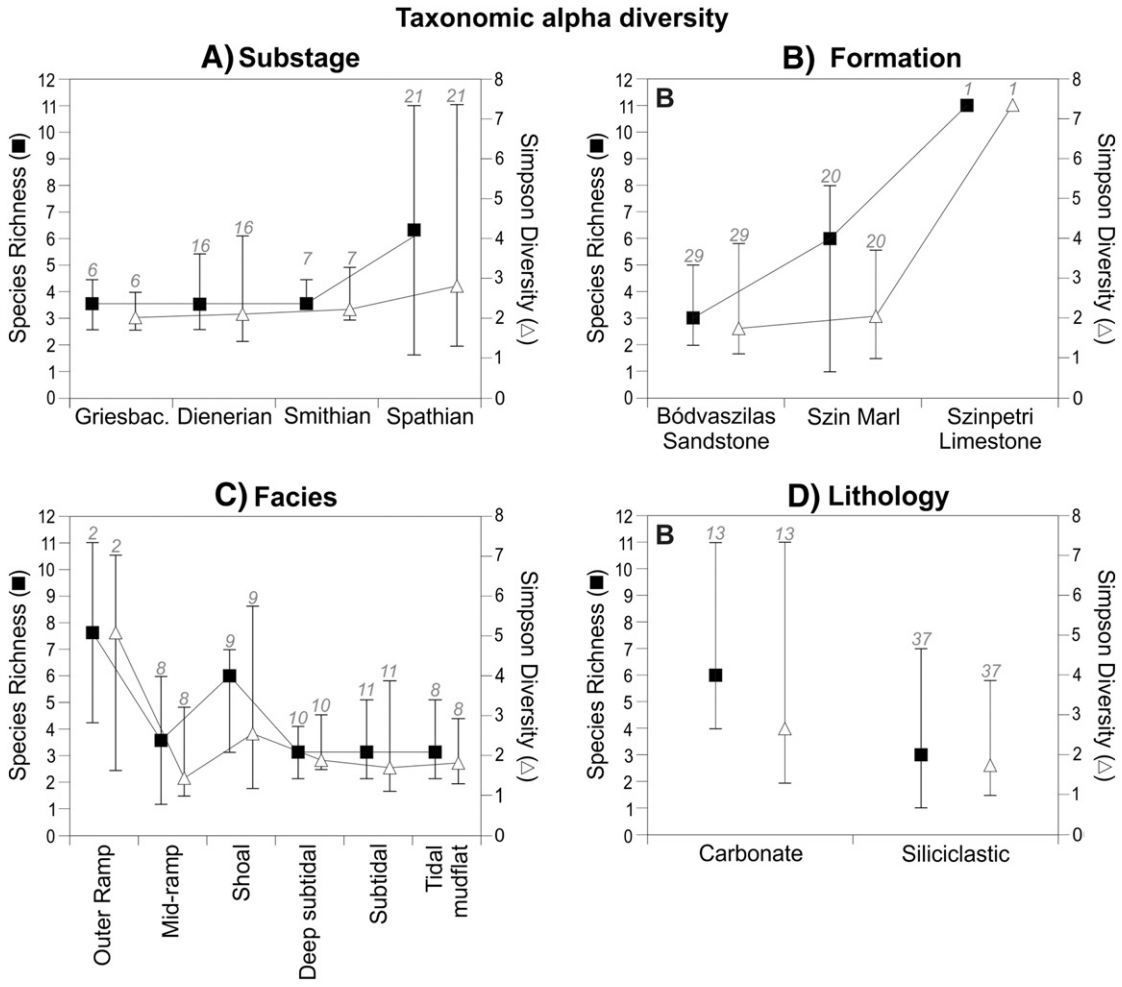

Fig. 6. Box plots showing the changes in alpha diversity. A) Sub-stage, B) formation, C) facies and D) lithology. Black squares represent median taxonomic richness and white triangle represents median Simpson Diversity. The maximum and minimum values are shown with short horizontal lines. Grey italics indicate the number of samples.

greater number of modes of life, do not (Fig. 11). The results of the PERMANOVA show that these differences are significant ($p = 0.001$), and the PERMDISP results show that the Griesbachian-Smithian Bódvaszilas Sandstone Formation samples are homogenous and it is not until the Spathian Szin Marl and Szinpetri Limestone formations that heterogeneity significantly increases (PERMDISP $p = 0.001$).

5. Ichnology

The trace fossils of the Lower Triassic succession have not been previously studied, although they are abundant at some levels. Eight ichnotaxa and wrinkle marks (sedimentary structures produced by microbial structures) were identified from this study (Fig. 12). The Bódvaszilas Sandstone Formation is characterised by low ichnogeneric diversity, small burrows and infrequent bioturbation. Ichnofabric indices (ii, Droser and Bottjer, 1986) of the Bódvaszilas Sandstone Formation are low (ii 1–2). No bioturbation was recorded in the Griesbachian strata, and Dienerian lower shoreface and tidal flat deposits were also almost undisturbed with only 1% of the thickness exhibiting weak (ii 2) bioturbation. In contrast, 30% of the Smithian strata are weakly (ii2) bioturbated (Fig. 13). Burrow diameters in the Bódvaszilas Sandstone Formation are small (average 3 mm; max. 7 mm; Fig. 13), average burrow depth is 19 mm (maximum 30 mm). In the Dienerian, only shallow-tier *Diplocraterion* and *Rhizocorallium jenense* were recorded, whereas in the Smithian *Skolithos* and *Arenicolites* were also present (Fig. 12). Wrinkle marks, on the other hand, were abundant throughout the entire Bódvaszilas Sandstone Formation.

The Spathian Szin Marl Formation records an increase in the ichnogeneric diversity and complexity but is also characterised by small burrow diameters (average 5 mm; max. 9 mm; Fig. 13), infrequent bioturbation (only 7% of the strata are (weakly) bioturbated (ii 2–3)) and the maximum burrow depth recorded was 50 mm. In the outer ramp facies no bioturbation was recorded (Fig. 14). In the mid-ramp facies seven ichnogenera were recognised: *Planolites*, *Rhizocorallium jenense*, *Diplocraterion*, *Catenichnus*, *Skolithos*, *Asteriacites* and an unidentified cubichnium. In contrast, in the shoal and protected inner ramp deposits only *Diplocraterion* and *Gyrochorte* were recorded (Fig. 14). The 'problematicum' of Hips (1996b) is identified as *Laevicyclus*, which occurs in the mid-ramp in Unit B of the Szin Marl Formation. The presence of *Gyrochorte* in inner ramp settings represents an increase in the complexity of trace fossil behaviour compared with the Bódvaszilas Sandstone Formation that lacked evidence for grazing activity.

The Szinpetri Limestone Formation records an expansion of bioturbation into the outer ramp environment, and major increases in the extent of bioturbation, burrow diameter and trace fossil complexity. Ninety-nine percent of the Szinpetri Limestone Formation is bioturbated, with 94% recording extensive (ii 4) bioturbation (Fig. 14). Four ichnogenera were recognised: *Thalassinoides*, *Planolites*, *Rhizocorallium irregulare* and the problematicum *Laevicyclus*. The first appearances of *R. irregulare* and, in particular, *Thalassinoides* indicate a major increase

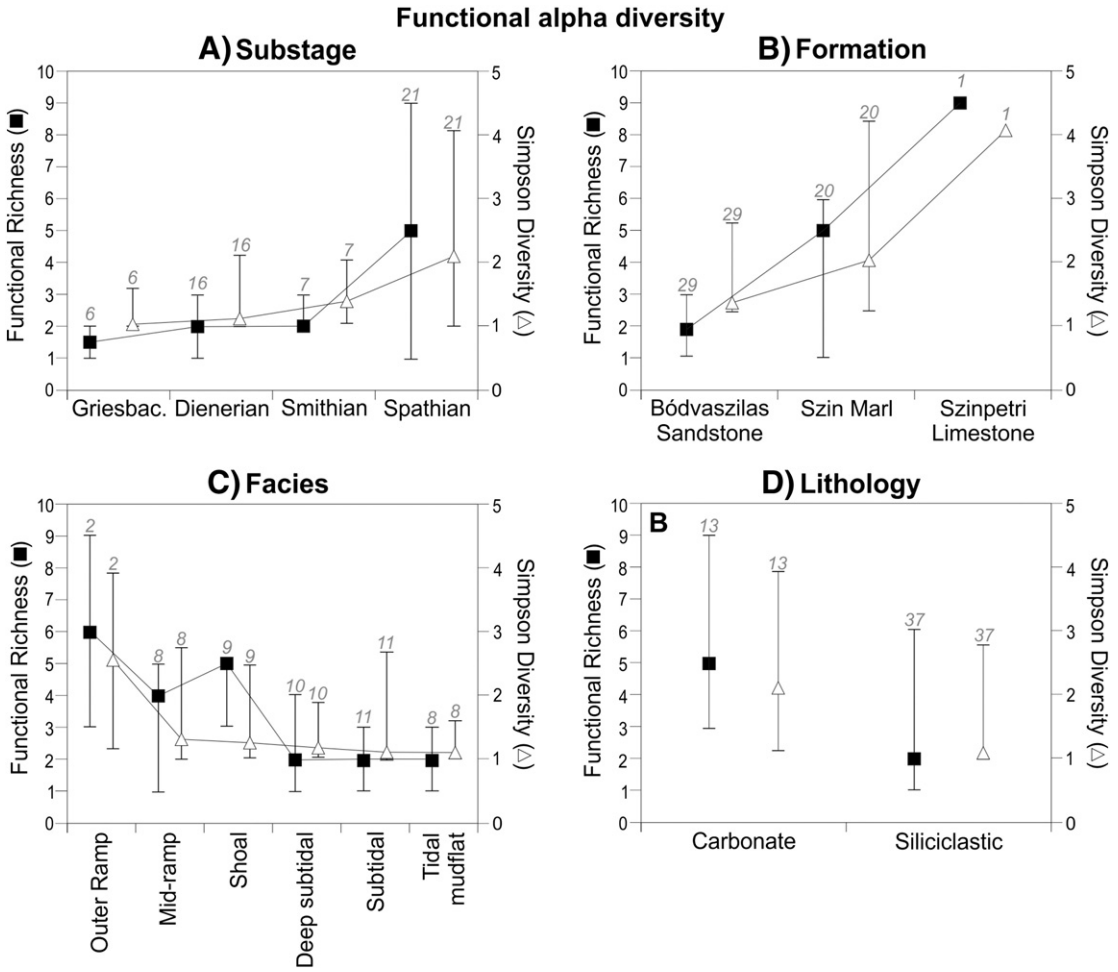

Fig. 7. Box plots showing the changes in functional alpha diversity. A) sub-stage, B) formation, C) facies and D) lithology. Black squares represent median functional richness and white triangle represents median Simpson Diversity. The maximum and minimum values are shown with short horizontal lines. Grey italics indicate the number of samples.

in the infaunal activity of crustaceans in the Lower Triassic succession of the Aggtelek Karst. Average burrow diameter is still small (6 mm), but maximum burrow diameter increases to 25 mm (Fig. 13). Burrow depth also increases in the Szinpetri Limestone Formation, but does not exceed 10 cm. The wrinkle marks that were recognised from tidal mudflat to outer ramp environments of the Bódvaszilas Sandstone and Szin Marl formations were not recorded in the Szinpetri Limestone Formation, suggesting that microbial mats had disappeared by the late Spathian.

6. Discussion

6.1. A delayed recovery of benthic marine ecosystems

Marine hypoxia and anoxia is often cited as a major control on the initial recovery of benthic marine communities following the late Permian extinction event (e.g. Twitchett et al., 2004). Previous studies have shown that in the absence of anoxia advanced stages of ecosystem recovery may be recorded locally by the second conodont zone, i.e. *Isarcicella isarcica* Zone, of the Induan (Twitchett et al., 2004). Outside the tropics, wave aeration of shallow marine environments above wave base is hypothesised to have created 'habitable zones' that enabled some survival and a rapid recovery during the Permian-Triassic oceanic anoxic event (Beatty et al., 2008; Zonneveld et al., 2010).

Initial deposition of the Bódvaszilas Sandstone Formation occurred during the late Griesbachian in an inner ramp environment that Hips (1996b) interpreted to have been reasonably well oxygenated. Sedimentology provides clear evidence of wave aeration and a potential habitable zone (Table 1) yet the benthic assemblages from these deposits have low alpha taxonomic ($S = 1$–2; $\Delta = 1$–1.6), low ecological diversities ($S = 1$–2; $\Delta = 1$–1.6), and low tiering. These data indicate that no significant ecological recovery had taken place and imply an additional environmental stress in the shallow, proximal settings of western Palaeotethys that was not mitigated by wave aeration.

In Neotethys, rapidly recovering benthic ecosystems collapsed to low evenness/low diversity skeletal assemblages at the end of the Griesbachian that led Twitchett et al. (2004) and Jacobsen et al. (2011) to infer a regional crisis related to marine transgression and seafloor anoxia. Stanley (2009) hypothesised that the late Griesbachian (mid-Induan) was a time of global biotic crisis, associated with transgression and regional anoxia (Wignall and Hallam, 1993), and negative carbon and oxygen isotope excursions (Payne et al., 2004; Sun et al., 2012). A decline in conodont and ammonoid diversity supports this hypothesis (Brayard et al., 2006; Orchard, 2007; Stanley, 2009). Our data demonstrate, however, that there were no significant differences in the composition, ecological structure or alpha diversity of shelly benthic marine assemblages across the Griesbachian/Dienerian boundary in the Bódvaszilas Sandstone Formation. The only recorded changes to the benthic ecosystem are the first appearances of *Diplocraterion* and short, obliquely oriented (~45°) *Rhizocorallium jenense* in the Dienerian. The appearance of these ichnotaxa, and their small size, represents a minor increase infaunal tiering and the return of suspension-feeding

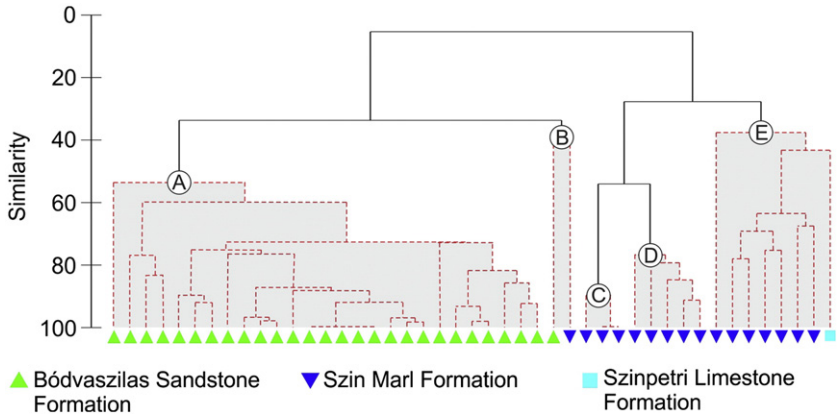

Fig. 8. Cluster analysis of the samples from the Lower Triassic succession of the Aggtelek Karst. The cluster analysis together with the SIMPROF test, identified 5 groups of samples which are statistically distinct (shaded area, dashed lines). The 5 groups have been interpreted as different benthic biofacies.

domichnia consistent with early recovery (Stage 2 of Twitchett et al., 2004; Twitchett, 2006).

The absence of a Late Griesbachian biotic crisis in the Aggtelek Karst (this study) and the Dolomites (Hofmann et al., 2015) indicates that it is not a global event, at least amongst the benthos. A critical aspect of the Hungarian record is that there is no facies change across the Griesbachian/Dienerian boundary. Localities in Neotethys that record a Late Griesbachian benthic biotic crisis, such as Wadi Wasit in Oman (Twitchett et al., 2004), also record a major change to deeper, more oxygen-restricted facies. In these locations, the supposed "crisis" may

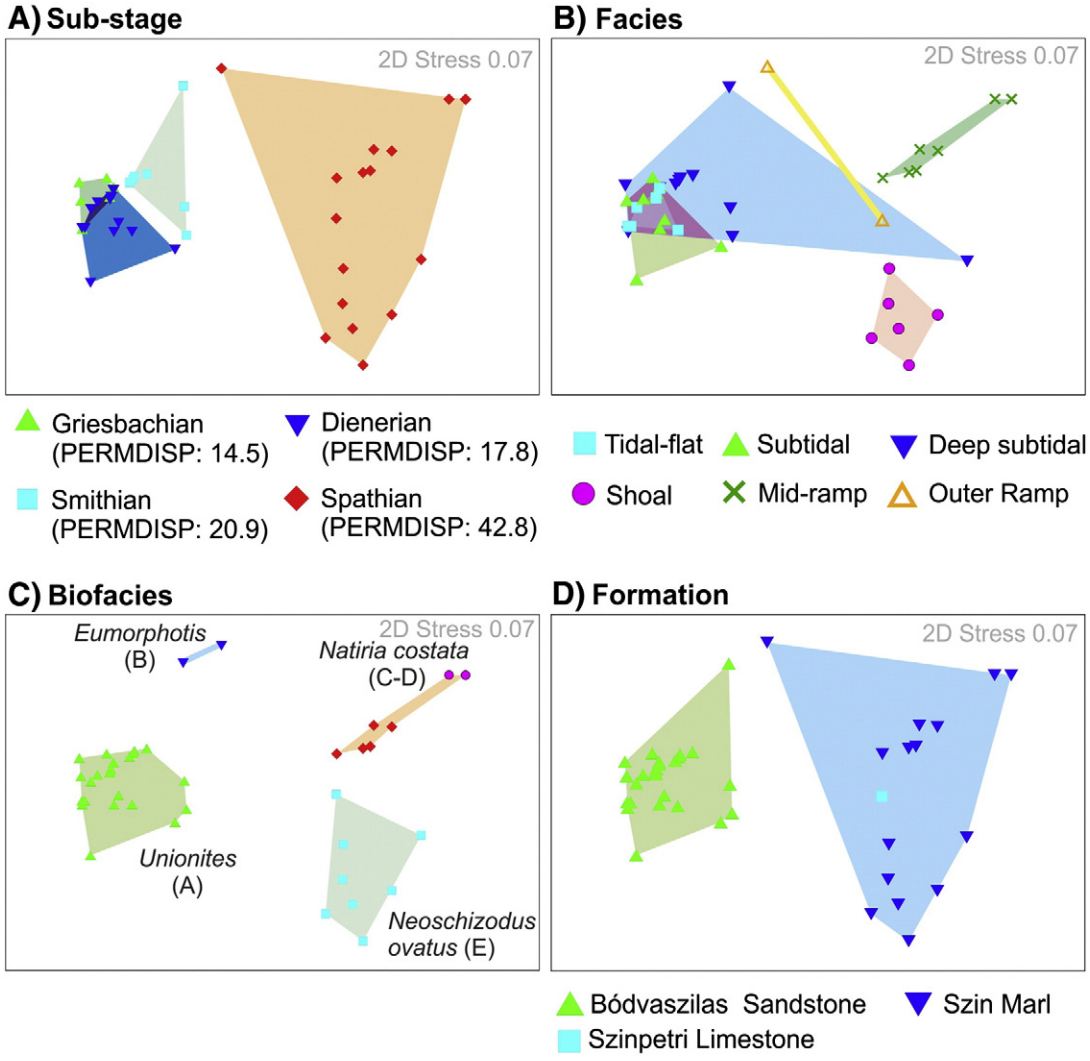

Fig. 9. Non-metric multi-dimensional scaling (nMDS) ordination of samples. A) samples are grouped according to sub-stage, B) samples are grouped according to lithofacies, C) samples are grouped according to biofacies and D) samples are grouped according to formation.

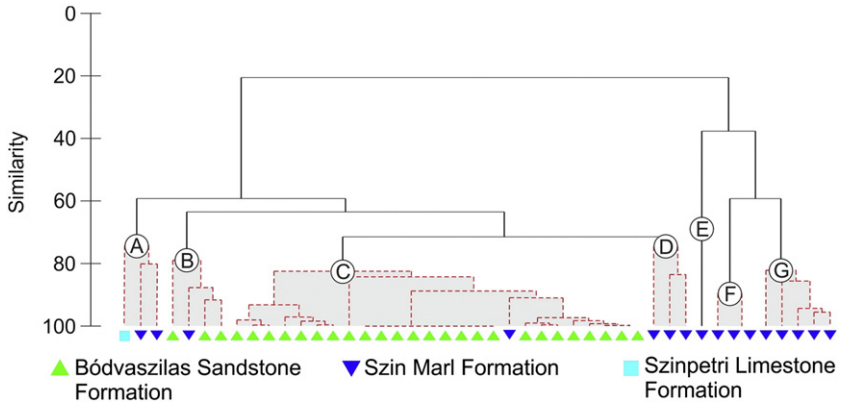

Fig. 10. Cluster analysis of modes of life from the Lower Triassic succession of the Aggtelek Karst. The cluster analysis together with the SIMPROF test, identified 7 groups of samples which are statistically distinct (A–G). The 7 groups have been interpreted as different functional biofacies.

simply reflect expected ecological change along an onshore-offshore diversity gradient and the successive sampling of shallower and then deeper benthic assemblages. This interpretation is supported by Hofmann et al. (2013b) study of the Griesbachian/Dienerian boundary of the Dinwoody Formation, USA, where high diversity/high evenness faunas were restricted to settings that were influenced by wave activity, i.e. the habitable zone, with low diversity/low evenness faunas in outer ramp environments.

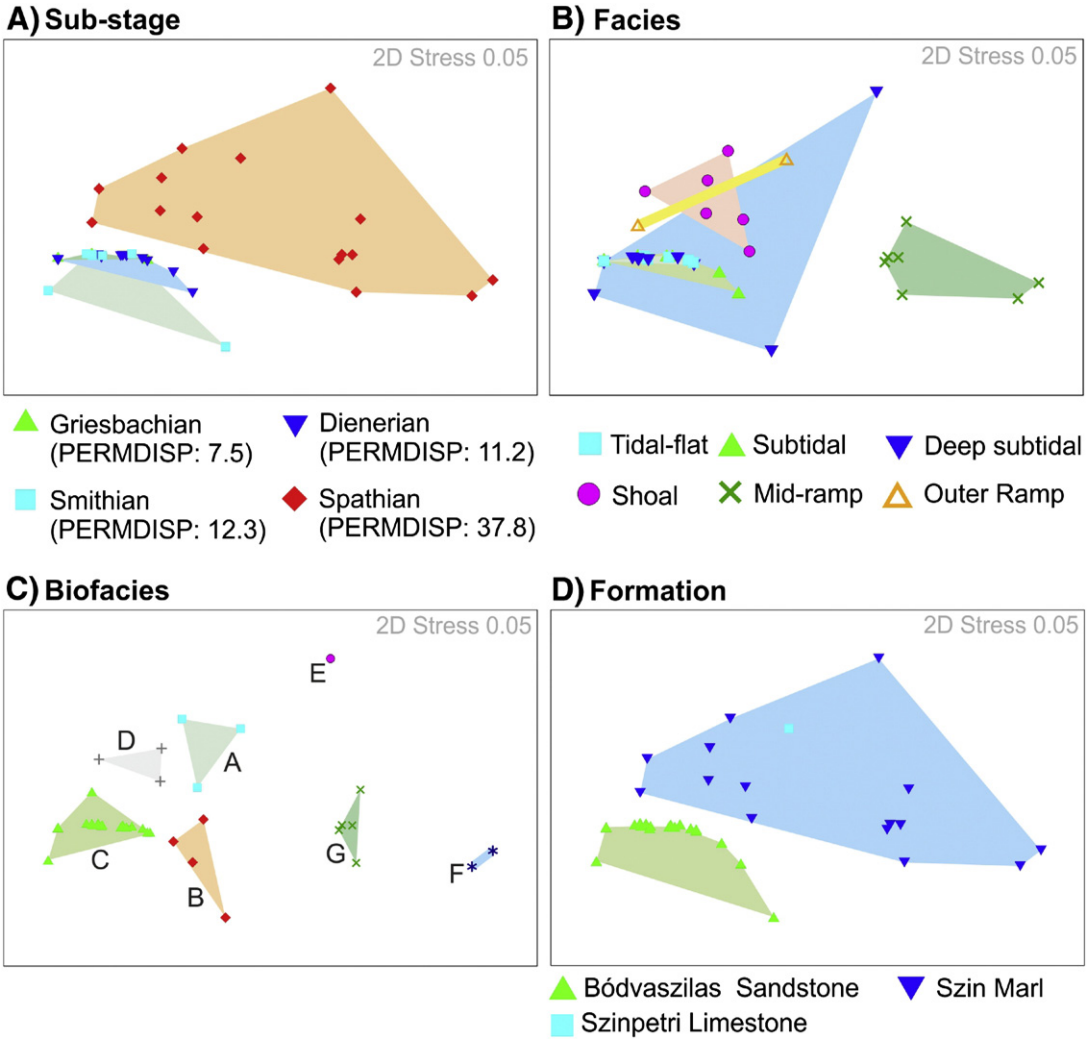

Fig. 11. Non-metric multi-dimensional scaling (nMDS) ordination for functional diversity of samples. A) Samples are grouped according to sub-stage, B) samples are grouped according to lithofacies, C) samples are grouped according to biofacies and D) samples are grouped according to formation.

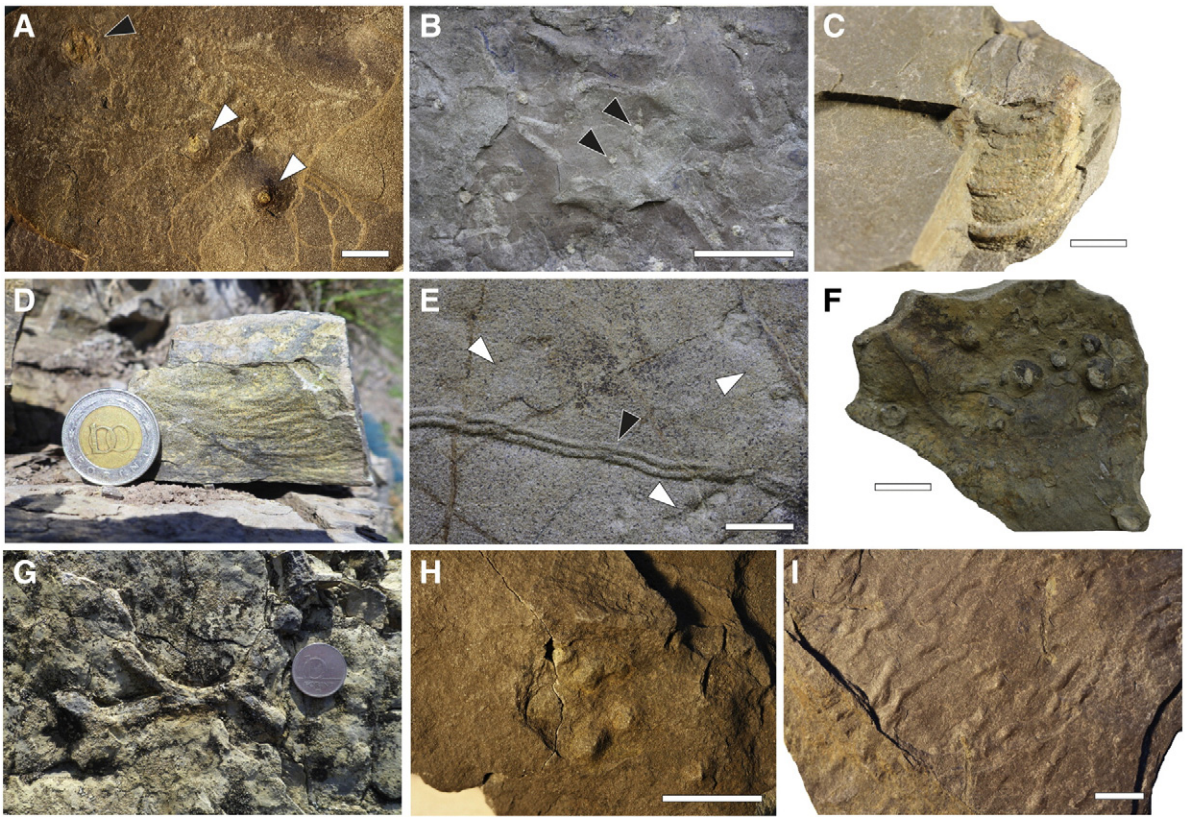

Fig. 12. Biosedimentary structures from the Lower Triassic of the Aggtelek Karst. A) *Arenicolites* (white arrow) and *Skolithos* (black arrow), Bódvaszilas Sandstone Formation. B) *Diplocraterion* (black arrow), Bódvaszilas Sandstone Formation. C) *Rhizocorallium jenense*, Bódvaszilas Sandstone Formation. D) *Diplocraterion*, Bódvaszilas Sandstone Formation. E) *Gyrochorte* (black arrow) and *Arenicolites* (white arrows), Unit D Szin Marl Formation. F) Unidentified cubichnia. Unit B Szin Marl Formation. G) *Thalassinoides*, Szinpetri Limestone Formation. H) *Asteriacites obtusus*, Unit B Szin Marl Formation. I) wrinkle marks, Bódvaszilas Sandstone Formation. Scale bar is 10 mm, coin is 10 mm.

6.2. Environmental stress in the habitable zone of western Palaeotethys

Based on the distribution of trace fossils, Beatty et al. (2008) limit the proximal end of the habitable zone to the upper shoreface to swash zone, where high turbidity and shifting sediments suppress benthic colonisation and reduce preservation potential. In the shallowest waters, especially in tropical latitudes such as that of the study site, benthic animals may also have been subjected to thermal stress (cf. Knoll et al., 2007). Other potential environmental stressors in shallow marine environments that may have excluded or restricted benthic invertebrates during the Early Triassic include large salinity fluctuations (Posenato, 1985, 2008b; Nützel and Schulbert, 2005); high sedimentation (Algeo and Twitchett, 2010); eutrophication (Algeo and Twitchett, 2010); desiccation stress (Petes et al., 2007); increased ocean surface pH and $CaCO_3$ saturation (Fraiser and Bottjer, 2007; Payne et al., 2011).

The benthic communities of the Bódvaszilas Sandstone Formation are characterised by the bivalve genera *Unionites*, *Eumorphotis* and *Claraia*, lingulid brachiopods and microconchids, which are frequently described as eurytopic opportunistic taxa that thrived in stressed environments in the wake of the late Permian mass extinction event (Schubert and Bottjer, 1995; Twitchett, 1999; Rodland and Bottjer, 2001; Posenato, 2008a; Hautmann et al., 2011; Fraiser, 2011; Zatoń et al., 2013; Posenato et al., 2014). Alternatively, the immediate post-extinction expansion of such opportunistic taxa may be a consequence of reduced competition, at least initially (cf. Harries et al., 1996). The lack of unequivocally stenohaline taxa suggests that salinities were outside the normal marine range during deposition of the Bódvaszilas Sandstone Formation. One consequence of global warming is an increase in runoff and evaporation (Labat et al., 2004), leading to greater salinity fluctuations in nearshore environments that would increase osmoregulation stress (Verschuren et al., 2000) and may have impeded the distribution of stenohaline animals, such as crinoids.

Increased weathering, sedimentation rates and run off would enhance nutrient supply to proximal shelf settings (Peizhen et al., 2001; Algeo and Twitchett, 2010) resulting in development of eutrophication in nearshore environments (Meyer et al., 2008; Schobben et al., 2015). The entire thickness of the Bódvaszilas Sandstone Formation in the Aggtelek Karst is not known due to faulting and folding, but its minimum thickness is 250 m (Hips, 1996b). The minimum average linear accumulation rate for the Griesbachian-Smithian interval is therefore, 187 m per myr, which is comparable to the elevated sedimentation rates recognised in shelf settings elsewhere during the Early Triassic (Algeo and Twitchett, 2010). In addition, abundant load structures throughout the Bódvaszilas Sandstone Formation suggest rapid, local sediment deposition. Eutrophication may negatively affect grazing animals as it provides unfavourable conditions for macrophytes, creating a shift in the communities of primary producers to microbial mats and free floating algae (Grall and Chauvaud, 2002). The Bódvaszilas Sandstone Formation contains abundant wrinkle structures, which confirm the widespread occurrence of microbial mats, and lacks evidence of grazers, which is consistent with the expected outcome of eutrophication. On the other hand, eutrophication may favour stationary suspension feeders that can tolerate seasonal hypoxia during calm water periods, as it increases the availability of food (Loo and Rosenberg, 1989; Carmichael et al., 2012). In the neighbouring Dolomites, northern Italy, an enrichment of $\delta^{34}S$ is observed in nearshore settings from the Griesbachian to Smithian (Horacek et al., 2010). The $\delta^{34}S$ signature at

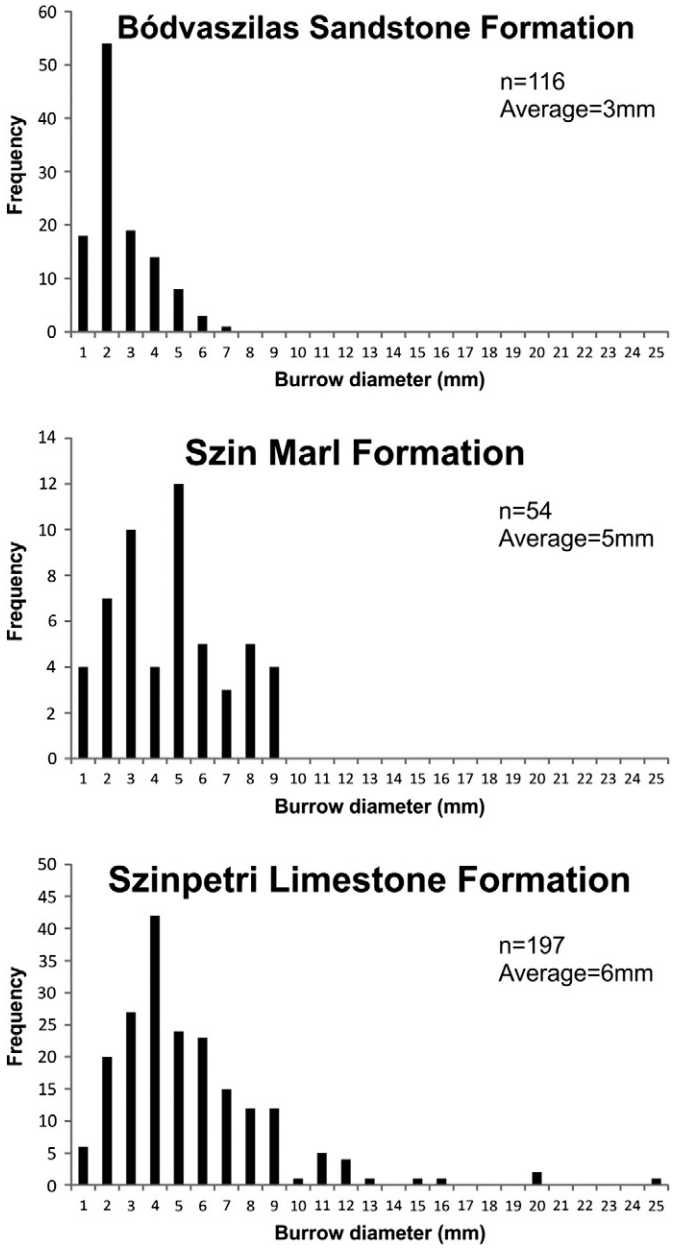

Fig. 13. Histograms of the burrow diameter of the Lower Triassic Formations of the Aggtelek Karst.

least partly reflects phosphorous recycling, which is vital for maintaining high primary productivity (Mort et al., 2007), this would provide additional support for the increase in primary productivity during the Griesbachian, Dienerian and Smithian.

Thus, in an interval of global warming, the nearshore, wave aerated habitable zone of tropical western Palaeotethys would be expected to subject to a number of potential stressors that would not be mitigated by wave aeration. Results of our sedimentological and palaeoecological analyses of the Bódvaszilas Sandstone Formation are consistent with the presence of at least some of these possible stressors.

A synergy of large salinity fluctuations, elevated sedimentation and eutrophication may therefore explain why the Bódvaszilas Sandstone exhibits low diversities and communities dominated by the cosmopolitan suspension-feeding, epifaunal bivalves *Unionites*, *Claraia* and *Eumorphotis*, and a shallow infaunal, suspension-feeding, non-mineralised benthos that lived in vertical or steeply inclined U-shaped burrows (*Diplocraterion* and *Rhizocorallium jenense*). Similar benthic communities are found in coeval tropical shelf settings elsewhere in western Palaeotethys (Broglio Loriga et al., 1990; Twitchett, 1999; Šimo and Olšavskỳ, 2007; Hofmann et al., 2015) and more widely (Schubert and Bottjer, 1995; Wignall et al., 1998; Hofmann et al., 2013b; Pietsch et al., 2014) suggesting that many nearshore, wave-aerated habitats probably experienced similar stressful conditions at times during the Lower Triassic.

6.3. Spathian recovery

Globally, the Spathian marks an advanced recovery phase for the benthos following the late Permian extinction event, with increasing diversity, re-establishment of deep and erect tiers, and evidence of increased predation (Schubert and Bottjer, 1995; Twitchett, 1999, 2006; Twitchett et al., 2004; Posenato, 2008a; Hofmann et al., 2013a, 2014, 2015). This global pattern is reflected locally by the Spathian Szin Marl faunas, which record significantly greater richness and the reestablishment of erect and deep infaunal tiers. The taxa *Holocrinus* and cf. *Pholadomya* sp. that, respectively, represent these tiers are, however, relatively small and thus did not occupy the full range of available space above and below the sediment-water interface as recorded in the Anisian (Hagdorn and Velledits, 2006; Fig. 15). In addition, cf. *Pholadomya* sp. has only been recorded in Unit C of the Szin Marl Formation suggesting that it is restricted to wave agitated environments. Disarticulated *Holocrinus* ossicles have been identified from the mid- to outer ramp (Hips, 1996b), but their original living habitat is hard to determine because their small size and robustness makes them easy to transport over large distances (Baumiller, 2001). Crinoid ossicles from the Szin Marl Formation are only found in storm beds suggesting that their living habitat may have been restricted to settings above wave base, i.e. the habitable zone.

The Spathian recovery signal is likely due, at least in part, to a greater number of facies in the Szin Marl Formation. Prior to the Spathian, only facies from stressed inner and mid-ramp environments were sampled. Inner ramp settings represented by units A and D of the Szin Marl Formation still reflect high stress, as inferred from low ichnofabric indices (Fig. 14), and no body fossils were recovered from these units to compare with the Bódvaszilas Sandstone Formation. The lack of bioturbation and a similar lithofacies to the Bódvaszilas Sandstone Formation suggests that those conditions limiting benthic recovery in the Bódvaszilas Sandstone Formation continued into the Spathian. The rest of the Szin Marl Formation, on the other hand, records strong habitat differentiation with different biofacies representing each sedimentary facies. This compares with the Spathian rocks from the western USA (Hofmann et al., 2013a, 2014). The most diverse assemblages are associated with oolitic shoals, and these habitats are not recorded prior to the Spathian in the Aggtelek Karst. Faunal changes in mid- and outer ramp settings from the Griesbachian to Smithian are currently unknown, and the onset of local recovery in those environments may have possibly occurred prior to the Spathian.

The high diversity reported in shoal and mid-ramp environments is consistent with a 'habitable zone' between the lower shoreface and offshore transition as recorded in the Sverdrup Basin, Canada (Beatty et al., 2008; Zonneveld et al., 2010) and in the Virgin Limestone Formation, western USA (Mata and Bottjer, 2011). Deposits distal to this habitable zone are characterised by low taxonomic and ecological diversities in the USA and Canada. Benthic faunas in Aggtelek do not appear in the settings below wave base until the late Spathian. The absence of benthic life below wave base is attributed to persistent, or very frequently recurring, environmental stress as it has been shown in the modern that once harsh environmental conditions (e.g. local anoxia) have ameliorated local benthic ecosystems recover within at most a few years (e.g. Boesch and Rosenberg, 1981; Diaz and Rosenberg, 1995, 2008). However, all modern examples involve a pool of potential colonisers in relatively close proximity, and it is possible that the geographic and taxonomic scale of the late Permian extinction may also have impacted

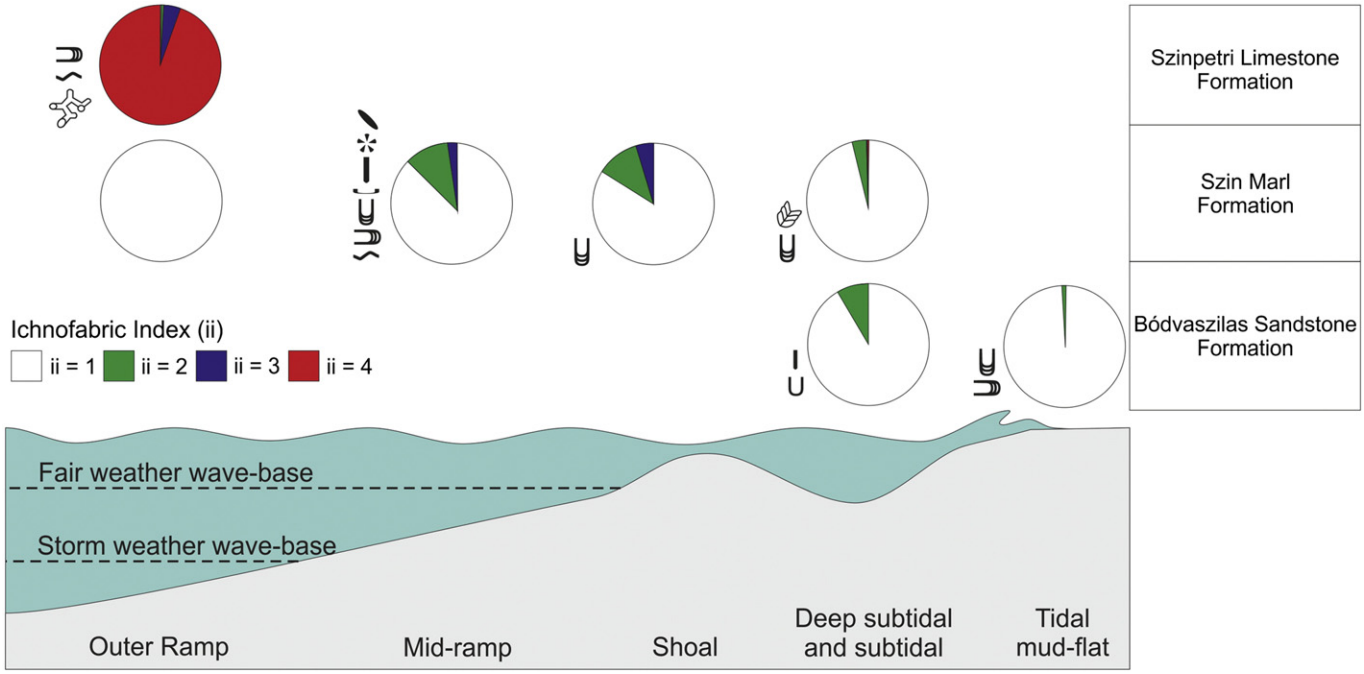

Fig. 14. Proportion of bioturbated sediment between the different Lower Triassic formations of the Aggtelek Karst and the distribution of trace fossils. Figures of trace fossils are same as Fig. 3.

the rates of local recolonization. The high resemblance between the fauna of Szinpetri Limestone and shallower settings of the Szin Marl Formation suggests that the fauna that colonised the outer ramp in the *T. carniolicus* Zone were previously restricted to shallower settings.

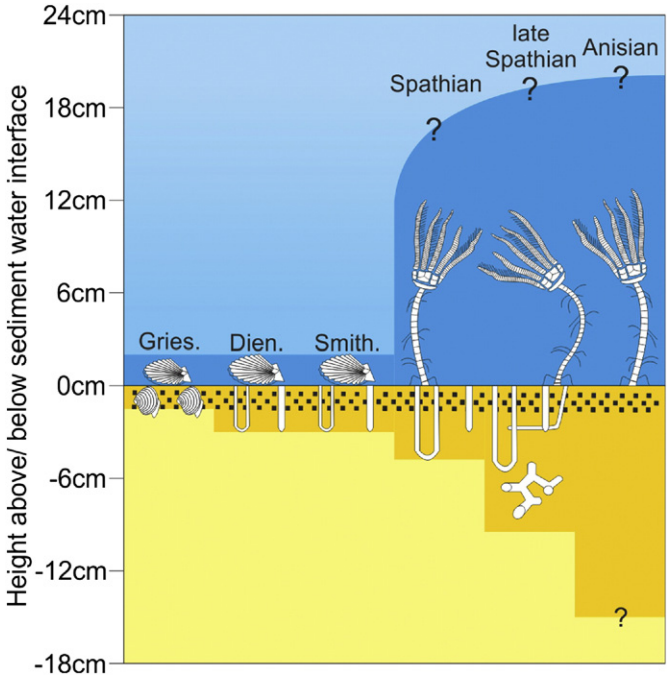

Fig. 15. Tiering above and below the sediment-water interface following the late Permian mass extinction in the Aggtelek Karst. Question marks refer to the uncertainty concerning the height of *Holocrinus* as no complete specimens have been found. Tiering in the Anisian is taken from Hagdorn and Velledits (2006) and Baumiller and Hagdorn (1995) for the erect tier and the German Muschelkalk for the infaunal tier (Knaust, 2007). Gries. = Griesbachian, Dien = Dienerian, Smith = Smithian. Note: increase in erect tiering between the Spathian and Anisian is inferred from an increase in the diameter of crinoid ossicles from the Aggtelek Karst.

6.4. Late Spathian recovery pulse

Only a single sample was recovered from the late Spathian Szinpetri Limestone Formation, yet this sample had the highest alpha diversity values of all studied samples. Compared to the outer ramp sample from Unit F of the Szin Marl Formation from the same facies, this sample records higher alpha diversity, both taxonomically and ecologically, and includes skeletal groups associated with advanced recovery, i.e. crinoids. Bioturbation intensity rises to levels (ii4–5) not recorded elsewhere in the Aggtelek Lower Triassic succession, and the occurrences of *Thalassinoides* and *Rhizocorallium irregulare*, which represent crustacean activity, indicate advanced recovery (cf. Twitchett and Barras, 2004; Twitchett, 2006). Advanced recovery in the late Spathian has also been observed globally with increased burrow sizes in northern Italy (Twitchett and Wignall, 1996; Twitchett, 2007), south China (Chen et al., 2011) and Svalbard (Worsley and Mørk, 2001); increased burrow depths (Twitchett, 1999); intense bioturbation in northern Italy (Twitchett and Wignall, 1996; Twitchett and Barras, 2004) and the Bükk Mountains, Hungary (Hips and Pelikán, 2002); conifer-dominated forests on land (Looy et al., 1999); the establishment of reefs on the Great bank of Guizhou, China (Payne et al., 2006b) and, *Placunopsis* bioherms in western USA (Pruss et al., 2007).

Globally, these advances in ecological recovery in the late Spathian coincide with an increase in the δ^{18} oxygen isotope record (Sun et al., 2012; Romano et al., 2012) that either reflects a decline in temperature or a change from low to normal salinity, or both. The subsequent re-establishment of strong latitudinal temperature gradients (Brayard et al., 2006) and oxic conditions in the outer ramp (Grasby et al., 2013) are related to improved ocean circulation. This would have led to a retreat of the oxygen minimum zone and expansion of potentially habitable area into the outer shelf environment. The fossil assemblages of the Szinpetri Limestone have a similar structure to those of the oolitic shoal and mid-ramp settings of the underlying Szin Marl Formation (Fig. 13), and have faunal elements (i.e. *Costatoria costata*) in common with the outer ramp setting of the Szin Marl Formation. This suggests that the benthic fauna from shallower settings rapidly colonised the outer ramp environment once it became better oxygenated, and

supports the hypothesis that rapid refilling of vacated seafloor by surviving taxa occurred before novel functional morphologies could evolve (Erwin et al., 1987; Foster and Twitchett, 2014). The recovery of benthic invertebrates recorded in this study area is limited mostly to molluscs and crinoids during the Lower Triassic, and recovery of other groups, (e.g. sponges, corals, echinoids and brachiopods) is not recorded locally until the Anisian (Hips, 2007; Velledits et al., 2011).

7. Conclusion

Our quantitative analyses show that fossil assemblages of the Induan (Griesbachian and Dienerian) and lower Olenekian (Smithian) of the Aggtelek Karst, which were deposited in nearshore, proximal ramp settings, have low diversity and low evenness and are exclusively represented by low tier, opportunistic, euryhaline taxa. Their palaeoecological characteristics are consistent with limited post-Permian recovery and persistent environmental stress. Although no fossiliferous samples were recorded from these nearshore settings in the Spathian, the lack of bioturbation in those facies suggests that this environment was still stressed during the *T. cassianus* Zone. Sedimentological and palaeoecological evidence, including the absence of grazers and stenohaline taxa and the abundance of wrinkle marks, are consistent with the presence of stressors such as large salinity fluctuations, high sedimentation rates, eutrophication and related oxygen-stress in proximal, nearshore settings of western Palaeotethys during the Induan and early Olenekian.

The Spathian Szin Marl Formation records increased species richness, changes in taxonomic composition, increased heterogeneity, stenohaline taxa and the appearance of deeper infaunal and erect epifaunal tiers. This is consistent with advanced ecological recovery, but is at least partly driven by an increased range of sampled facies and environments. The small body size of the Szin Marl fauna suggests that benthic communities were still stressed. These assemblages are all associated with facies that record the activity of waves, supporting the habitable zone hypothesis. In the *T. carniolicus* Zone, sample richness and bioturbation increase to levels not previously recorded. Globally, this is associated with climate cooling, the re-establishment of ocean circulation and retreat of the oxygen minimum zone creating an expanded habitable area which was rapidly filled by shallow water taxa.

Acknowledgements

WJF would like to thank Verity Macfarlane for her assistance in the field, and József Pálfy and Balint Petardi for their hospitality whilst visiting the Eötvös Loránd University and Hungarian Geological Institute respectively. Tatsuo Oji is also thanked for discussions on Early Triassic *Holocrinus*. An anonymous reviewer and Richard Hofmann are thanked for their constructive comments that improved the manuscript. This study was supported by a Natural Environment Research Council (NERC) grant (NE/I005641/1) to RJT.

Appendix A. $^{87}Sr/^{86}Sr$ methods and results

Bulk rock powders were generated by drill with a preference for micrite and an avoidance of bioclasts and secondary calcite veins. Approximately 40 mg of the resulting bulk rock powders were pre-treated with ultrapure 1 M ammonium acetate buffered to a pH of 8 (Montañez et al., 1996; Bailey et al., 2000), then leached in 4% acetic acid. The resulting supernatant was collected and spiked with an ^{84}Sr tracer. Sr was isolated using Biorad AG 50 × 8 cation exchange resin and a 2 N HCl based ion exchange following the laboratory methods of Foland and Allen (1991). Samples were loaded with HCl on a Re double filament configuration with a Ta_2O_5 activator. Isotopic compositions were measured with a Finnegan MAT 261A thermal ionization mass spectrometer at The Ohio State University. The laboratory reproducibility of the standard SRM 987 is 0.710242 ± 0.000010 (1σ reproducibility). Reported $^{87}Sr/^{86}Sr$ values are corrected for instrumental fractionation using normal $^{86}Sr/^{88}Sr$ of 0.119400.

A.1. Results

Locality	Formation	Log height (m)	$^{87}Sr/^{86}Sr$	Sr ppm	Uncertainty
Perkupa Cemetery	Bódvaszilas Sandstone	1.0	0.709719	171.0	0.000010
Perkupa West	Szin Marl	0.3	0.708366	403.6	0.000012
Perkupa Vineyard	Szin Marl	17.3	0.708396	562.1	0.000009
Szinpetri Quarry	Szin Marl	1.0	0.708440	403.4	0.000015
Szin North	Szinpetri Limestone	26.0	0.708162	3934.4	0.000010

Appendix B. Supplementary data

Supplementary data to this article can be found online at http://dx.doi.org/10.1016/j.palaeo.2015.09.004.

References

Algeo, T.J., Twitchett, R.J., 2010. Anomalous Early Triassic sediment fluxes due to elevated weathering rates and their biological consequences. Geology 38, 1023–1026.
Anderson, M.J., 2001. A new method for non-parametric multivariate analysis of variance. Austral Ecol. 26, 32–46.
Anderson, M.J., Gorley, R.N., Clarke, R.K., 2008. PERMANOVA + for PRIMER: guide to software and statistical methods. PRIMER-E, Plymouth, UK.
Bailey, T.R., McArthur, J.M., Prince, H., Thurwall, M.F., 2000. Dissolution methods for strontium isotope stratigraphy: whole rock analysis. Chem. Geol. 167, 313–319.
Bambach, R.K., Bush, A.M., Erwin, D.H., 2007. Autecology and the filling of ecospace: key metazoan radiations. Palaeontology 50, 1–22.
Baumiller, T.K., 2001. Experimental and biostratinomic disarticulation of crinoids; taphonomic implications. In: Féral, J.-P., David, B. (Eds.), Echinoderm Research. Swets and Zeitlinger Lisse, Netherlands, pp. 243–248.
Baumiller, T.K., Hagdorn, H., 1995. Taphonomy as a guide to functional morphology of *Holocrinus*, the first pose-Paleozoic crinoid. Lethaia 28, 221–228.
Beatty, T.W., Zonneveld, J.-P., Henderson, C.M., 2008. Anomalously diverse Early Triassic ichnofossil assemblages in Northwest Pangea: a case for a shallow-marine habitable zone. Geology 36, 771–774.
Benton, M.J., Twitchett, R.J., 2003. How to kill (almost) all life: the end-Permian extinction event. Trends Ecol. Evol. 18, 358–365.
Blakey, R., 2012. Global Paleogeography. http://www2.nau.edu/rcb7/globaltext2.html.
Boesch, D.F., Rosenberg, R., 1981. Response to stress in marine benthic communities. In: Barrett, G.W., Rosenberg, R. (Eds.), Stress Effects On Natural Ecosystems. Wiley, New York, pp. 177–196.
Brayard, A., Bucher, H., Escarguel, G., Fluteau, F., Bourquin, S., Galfetti, T., 2006. The Early Triassic ammonoid recovery: paleoclimatic significance of diversity gradients. Palaeogeogr. Palaeoclimatol. Palaeoecol. 239, 374–395.
Broglio Loriga, C., Mirabella, S., 1986. Il genere *Eumorphotis* Bittner 1901 nella biostratigrafia dello Scitico, Formazione di Werfen (Dolomiti). Sci. Geol. Mem. 38, 245–281.
Broglio Loriga, C., Masetti, D., Neri, C., 1983. La formazione di Werfen (Scitico) delle Dolomiti Occidentali: sedimentologia e biostratigrafia. Riv. Ital. Paleontol. Stratigr. 88, 501–598.
Broglio Loriga, C., Posenato, R., 1986. Costatoria (Costatoria?) subrotunda (Bittner, 1901) a Smithian (Lower Triassic) marker from Tethys. Rivista Italiana di Paleontologia e Stratigrafia 92, 89–200.
Broglio Loriga, C., Góczán, F., Haas, J., Lenner, K., Neri, C., Oravecz-Scheffer, A., Posenato, R., Szaboacute, I., Tóth Makk, A., 1990. The Lower Triassic sequence of the Dolomites (Italy) and Transdanubian Mid-Mountains (Hungary) and their correlation. Sci. Geol. Mem., Padova 42, 41–103.
Bush, A.M., Bambach, R.K., Daley, G.M., 2007. Changes in theoretical ecospace utilization in marine fossil assemblage between the mid-Paleozoic and late Cenozoic. Paleobiology 33, 76–97.
Carmichael, R.H., Shriver, A.C., Valiela, I., 2012. Bivalve response to estuarine eutrophication: the balance between enhanced food supply and habitat alterations. J. Shellfish Res. 31, 1–11.
Chen, Z.-Q., Shi, G.R., Kaiho, K., 2004. New ophiuroids from the Permian/Triassic boundary beds of south China. Palaeontology 47, 1301–1312.
Chen, Z.-Q., Tong, J., Fraiser, M.L., 2011. Trace fossil evidence for restoration of marine ecosystems following the end-Permian mass extinction in the Lower Yangtze region, South China. Palaeogeogr. Palaeoclimatol. Palaeoecol. 299, 449–474.
Clarke, K.R., 1993. Non-parametric multivariate analyses of changes in community structure. Aust. J. Ecol. 18, 117–143.

Clarke, K.R., Gorley, R.N., 2006. *PRIMER v6*: User Manual/Tutorial. PRIMER-E, Plymouth.

Clarke, K.R., Warwick, R.M., 2001. Change In Marine Communities: An Approach To Statistical Analysis And Interpretation. 2nd edition. PRIMER-E, Plymouth.

Cox, L.R., et al., 1969. Treatise on Invertebrate Paleontology. Part N.Mollusca 6: Bivalvia. Geological Society of America and University of Kansas Press, USA.

Csontos, L., Vörös, A., 2004. Mesozoic plate tectonic reconstruction of the Carpathian region. Palaeogeogr. Palaeoclimatol. Palaeoecol. 210, 1–56.

Diaz, R.J., Rosenberg, R., 1995. Marine benthic hypoxia: a review of its ecological effects and the behavioural responses of benthic macrofauna. Oceanogr. Mar. Biol. Annu. Rev. 33, 245–303.

Diaz, R.J., Rosenberg, R., 2008. Spreading Dead Zones and consequences for marine ecosystems. Science 321, 926–929.

Droser, M.L., Bottjer, D.J., 1986. A semiquantitative field classification of ichnofabric: research method paper. J. Sediment. Res. 56, 558–559.

Erwin, D.H., Pan, H.-Z., 1996. Recoveries and radiations: gastropods after the Permo-Triassic mass extinction. In: Hart, M.B. (Ed.), Geological Society Special Publication No.102, pp. 223–229.

Erwin, D.H., Valentine, J.W., Sepkoski, J.J., 1987. A comparative study of diversification event; the early Paleozoic versus the Mesozoic. Evolution 41, 1177–1186.

Foland, K.A., Allen, J.C., 1991. Magma sources for Mesozoic anorogenic granites of the White Mountain magma series, New England, USA. Contrib. Mineral. Petrol. 109, 195–211.

Foster, W.J., Twitchett, R.J., 2014. Functional diversity of marine ecosystems following the late Permian mass extinction event. Nat. Geosci. 8, 233–238.

Fraiser, M.L., 2011. Paleoecology of secondary tierers from Western Pangaean tropical marine environments during the aftermath of the end-Permian mass extinction. Palaeogeogr. Palaeoclimatol. Palaeoecol. 308, 181–189.

Fraiser, M.L., Bottjer, D.J., 2004. The non-actualistic early Triassic gastropod fauna: a case study of Lower Triassic Sinbad Limestone Member. Palaios 19, 259–275.

Fraiser, M.L., Bottjer, D.J., 2007. Elevated atmospheric CO_2 and the delayed biotic recovery from the end-Permian mass extinction. Palaeogeogr. Palaeoclimatol. Palaeoecol. 252, 164–175.

Glazek, J., Radwański, A., 1968. Determination of brittle star vertebrae in thin sections. Acad. Pol. Sci. Bull. Sér. Sci. Géol. Géogr. 16, 91–96.

Grall, J., Chauvaud, L., 2002. Marine eutrophication and benthos: the need for new approaches and concepts. Glob. Chang. Biol. 8, 813–830.

Grasby, S.E., Beauchamp, B., Sembry, H.S., 2013. Recurrent Early Triassic ocean anoxia. Geology 41, 175–178.

Hagdorn, H., Velledits, F., 2006. Middle Triassic crinoid remains from the Aggtelek platform (NE Hungary). N. Jb. Geol. Paläont. 240, 373–404.

Hallam, A., 1991. Why was there a delayed radiation after the end-Palaeozoic extinctions? Hist. Biol. 5, 257–262.

Hammer, O., Harper, D.A.T., Ryan, P.D., 2001. PAST: Paleontological Statistics software package for education and data analysis. Palaeontol. Electron. 4, 1–9.

Harries, P.J., Kauffman, E.G., Hansen, T.A., 1996. Models for biotic survival following mass extinction. In: Hart, M.B. (Ed.), Biotic Recovery From Mass Extinction Events. Geological Society Of London Special Publications 102, pp. 41–60.

Hautmann, M., Bucher, H., Brühwiler, T., Goudemand, N., Kaim, A., Nützel, A., 2011. An unusually diverse mollusc fauna from the earliest Triassic of South China and its implications for benthic recovery after the end-Permian biotic crisis. Geobios 44, 71–85.

Hips, K., 1996a. The biostratigraphic significance of the *Cyclogyra–Rectocornuspira* association (Foraminifera; Early Triassic): data from the Aggtelek Mountains (Northeastern Hungary). N. Jb. Geol. Paläont. 7, 439–451.

Hips, K., 1996b. Stratigraphic and facies evaluation of the Lower Triassic formations in the Aggtelek–Rudabánya Mountains, NE Hungary. Acta Geol. Hung. 39, 369–411.

Hips, K., 1998. Lower Triassic storm-dominated ramp sequence in northern Hungary: an example of evolution from homoclinal through distally steepened ramp to Middle Triassic flat-topped platform. In: Wright, V.P., Burchette, T.P. (Eds.), Carbonate Ramps. Geological Society, London, Special Publications, 149, pp. 315–338.

Hips, K., 2007. Facies pattern of western Tethyan Middle Triassic black carbonates: the example of Gutenstein Formation in Silica Nappe, Carpathians, Hungary, and its correlation to formations of adjoining areas. Sediment. Geol. 194, 99–114.

Hips, K., Pelikán, P., 2002. Lower Triassic shallow marine succession in the Bükk Mountains, NE Hungary. Geol. Carpath. 53, 351–367.

Hofmann, R., Goudemand, N., Wasmer, M., Bucher, H., Hautmann, M., 2011. New trace fossil evidence for an early recovery signal in the aftermath of the end-Permian mass extinction. Palaeogeogr. Palaeoclimatol. Palaeoecol. 310, 216–226.

Hofmann, R., Hautmann, M., Wasmer, M., Bucher, H., 2013a. Palaeoecology of the Spathian Virgin Formation (Utah, USA) and its implications for the Early Triassic recovery. Acta Palaeontol. Pol. 58, 149–173.

Hofmann, R., Hautmann, M., Bucher, H., 2013b. A new paleoecological look at the Dinwoody Formation (Lower Triassic, western USA): intrinsic versus extrinsic controls on ecosystem recovery after the end-Permian mass extinction. J. Paleontol. 87, 854–880.

Hofmann, R., Hautmann, M., Brayard, A., Nützel, A., Bylund, K., Jenks, J.F., Vennin, E., Olivier, N., Bucher, H., 2014. Recovery of benthic marine communities from the end-Permian mass extinction at the low latitudes of eastern Panthalassa. Palaeontology 57, 1–43.

Hofmann, R., Hautmann, M., Bucher, H., 2015. Recovery dynamics of benthic marine communities from the Lower Triassic Werfen Formation, northern Italy. Lethaia. http://dx.doi.org/10.1111/let.12121.

Horacek, M., Brandner, R., Richoz, S., Povoden-Karadeniz, E., 2010. Lower Triassic sulphur isotope curve of marine sulphates from the Dolomites, N-Italy. Palaeogeogr. Palaeoclimatol. Palaeoecol. 290, 65–70.

Jacobsen, N.D., Twitchett, R.J., Krystyn, L., 2011. Palaeoecological methods for assessing marine ecosystem recovery following the late Permian mass extinction event. Palaeogeogr. Palaeoclimatol. Palaeoecol. 308, 200–212.

Jost, L., 2006. Entropy and diversity. Oikos 113, 363–375.

Kashiyama, Y., Oji, T., 2004. Low-diversity shallow marine benthic fauna from the Smithian of northeast Japan: paleoecologic and paleobiogeographic implications. Paleontol. Res. 8, 199–218.

Knaust, D., 2007. Invertebrate trace fossils and ichnodiversity in shallow-marine carbonates of the German Middle Triassic (Muschelkalk). SEPM Special Publications No.88pp. 221–238.

Knoll, A.H., Bambach, R.K., Payne, J.L., Pruss, S., Fischer, W.W., 2007. Paleophysiology and end-Permian mass extinction. Earth Planet. Sci. Lett. 256, 295–313.

Kolar-Jurkovšek, Vuks, V.J., Aljinovic, D., Hautmann, M., Kaim, A., Jurkovšek, B., 2013. Olenekian (Early Triassic) fossil assemblage from eastern Julian Alps (Slovenia). Ann. Soc. Geol. Pol. 83, 213–227.

Korte, C., Kozur, H.W., Bruckschen, P., Veizer, J., 2003. Strontium isotope evolution of Late Permian and Triassic seawater. Geochim. Cosmochim. Acta 67, 47–62.

Kovács, S., Less, G.Y., Piros, O., Róth, L., 1989. Triassic formations of the Aggtelek–Rudabánya Mountains (Northeastern Hungary). Acta Geol. Hung. 32, 31–63.

Kovács, S., Sudar, M., Gădinaru, E., Hans-Jürgen, G., Karmata, S., Haas, J., Péro, C., Gaetani, M., Mello, J., Polák, M., Aljinović, D., Ogorelec, B., Kolar-Jurkovšek, T., Jurkovšek, B., Buser, S., 2011. Triassic evolution of the Tectonostratigraphic Units of the Circum-Pannonian region. Jahrb. Geol. Bundesanst. 151, 199–280.

Labat, D., Goddéris, Y., Probst, J.L., Guyot, J.L., 2004. Evidence for global runoff increase related to climate warming. Adv. Water Resour. 27, 631–642.

Loo, L.-O., Rosenberg, R., 1989. Bivalve suspension-feeding dynamics and benthic–pelagic coupling in eutrophicated marine bay. J. Exp. Mar. Biol. Ecol. 130, 253–276.

Looy, C.V., Brugman, W.A., Dilcher, D.L., Visscher, H., 1999. The delayed resurgence of equatorial forests after the Permian–Triassic ecologic crisis. PNAS 96, 13857–13862.

Ludvigsen, R., Westrop, S.R., Pratt, B.R., Tuffnell, P.A., Young, G.A., 1986. Dual biostratigraphy: zones and biofacies. Geosci. Can. 13, 139–154.

Mata, S.A., Bottjer, D.J., 2011. Origin of Lower Triassic microbialites in mixed carbonate–siliciclastic successions: ichnology, applied stratigraphy, and the end-Permian mass extinction. Palaeogeogr. Palaeoclimatol. Palaeoecol. 300, 158–178.

McGhee, G.R., Clapham, M.E., Sheehan, P.M., Bottjer, D.J., Droser, M.L., 2013. A new ecological-severity ranking of major Phanerozoic biodiversity crises. Palaeogeogr. Palaeoclimatol. Palaeoecol. 370, 260–270.

Meyer, K.M., Kump, L.R., Ridgwell, A., 2008. Biogeochemical controls on photic-zone euxinia during the end-Permian mass extinction. Geology 36, 747–750.

Montañez, I.P., Banner, J.L., Osleger, D.A., Borg, L.E., Bosserman, P.J., 1996. Integrated Sr isotope variations and sea-level history of Middle to Upper Cambrian platform carbonates: implications for the evolution of Cambrian seawater $^{87}Sr/^{86}Sr$. Geology 24, 917–920.

Mort, H.P., Adatte, T., Föllmi, K.B., Keller, G., Steinmann, P., Matera, V., Berner, Z., Stüben, D., 2007. Phosphorus and the roles of productivity and nutrient recycling during oceanic anoxic event 2. Geology 35, 483–486.

Nakazawa, K., 1977. On *Claraia* of Kashmir and Iran. J. Palaeontol. Soc. India 20, 191–204.

Neri, C., Posenato, R., 1985. New biostratigraphical data on uppermost Werfen Formation of western Dolomites (Trento, Italy). Mitt. Geol. Paläontol. Innsbruck 14, 83–107.

Nützel, A., 2005. A new Early Triassic gastropod genus and the recovery of gastropods from the Permian/Triassic extinction. Acta Palaeontol. Pol. 50, 19–24.

Nützel, A., Schulbert, C., 2005. Facies of two important Early Triassic gastropod lagerstätten: implications for diversity patterns in the aftermath of the end-Permian mass extinction. Facies 51, 480–500.

Olszewski, T.D., 2004. A unified mathematical framework for the measurement of richness and evenness within and among multiple communities. Oikos 104, 377–387.

Orchard, M.J., 2007. Conodont diversity and evolution through the latest Permian and early Triassic upheavals. Palaeogeogr. Palaeoclimatol. Palaeoecol. 252, 93–117.

Patzkowsky, M.E., Holland, S.M., 2012. Stratigraphic Paleobiology: Understanding the Distribution of Fossil Taxa in Time and Space. The University of Chicago Press, Chicago.

Payne, J.L., Clapham, M.E., 2012. End-Permian mass extinction in the oceans: an ancient analog for the twenty-first Century? Annu. Rev. Earth Planet. Sci. 40, 89–111.

Payne, J.L., Lehrmann, D.J., Wei, J., Orchard, M.J., Schrag, D.P., Knoll, A.H., 2004. Large perturbations of the carbon cycle during recovery from the end-Permian extinction. Science 305, 506–509.

Payne, J.L., Lehrmann, D.J., Wei, J., Knoll, A.H., 2006a. The pattern and timing of biotic recovery from the end-Permian extinction on the Great Bank of Guizhou, Guizhou Province, China. Palaios 21, 63–85.

Payne, J.L., Lehrmann, D.J., Christensen, S., Wei, J., Koll, A.H., 2006b. Environmental and biological controls on the initiation and growth of a Middle Triassic (Anisian) reef complex on the Great Bank of Guizhou, Guizhou Province, China. Palaios 21, 325–343.

Payne, J.L., Turchyn, A.V., Paytan, A., DePaolo, D.J., Lehrmann, D.J., Yu, M., Wei, J., 2011. Calcium isotope constraints on the end-Permian mass extinction. PNAS 107, 8543–8548.

Peizhen, Z., Molnar, P., Downs, W.R., 2001. Increased sedimentation rates and grain sizes 2–4 Myr ago due to the influence of climate change on erosion rates. Nature 410, 891–897.

Petes, L.E., Menge, B.A., Murphy, G.D., 2007. Environmental stress decreases survival, growth, and reproduction in New Zealand mussels. J. Exp. Mar. Biol. Ecol. 351, 83–91.

Pietsch, C., Mata, S.A., Bottjer, D.J., 2014. High temperature and low oxygen perturbations drive contrasting benthic recovery dynamics following the end-Permian mass extinction. Palaeogeogr. Palaeoclimatol. Palaeoecol. 399, 98–113.

Posenato, R., 1985. Un'Associazione oligotipica a Neoschizodus ovatus (GOLDFUSS) della formazione di Werfen (Triassico INF-Dolomiti). Atti 3rd Symposia di ecologia e paleoecologia delle comunita bentoniche, Catania-Taormina 1985.

Posenato, R., 1992. Tirolites (Ammonoidea) from the Dolomites, Bakony and Dalmatia: taxonomy and biostratigraphy. Eclogae Geol. Helv. 85, 893–929.

Posenato, R., 2002. Bivalves and other macrobenthic fauna from the Ladinian "Muschelkalk" of Punta del Lavatoio (Alghero, SW Sardinia). Rend. Soc. Paleontol. Ital. 1, 185–196.

Posenato, R., 2008a. Patterns of bivalve biodiversity from Early to Middle Triassic in the Southern Alps (Italy): regional vs. global events. Palaeogeogr. Palaeoclimatol. Palaeoecol. 261, 145–159.
Posenato, R., 2008b. Global correlations of mid Early Triassic events: the Induan/Olenekian boundary in the Dolomites (Italy). Earth Sci. Rev. 91, 93–105.
Posenato, R., Holmer, L.E., Prinoth, H., 2014. Adaptive strategies and environmental significance of lingulid brachiopods across the late Permian extinction. Palaeogeogr. Palaeoclimatol. Palaeoecol. 399, 373–384.
Pruss, S.B., Payne, J.L., Bottjer, D.J., 2007. Placunopsis bioherms: the first metazoan buildups following the end-Permian mass extinction. Palaios 22, 17–23.
Rodland, D.L., Bottjer, D.J., 2001. Biotic recovery from the end-Permian mass extinction: behavior of the inarticulate brachiopod *Lingula* as a disaster taxon. Palaios 16, 95–101.
Romano, C., Goudemand, N., Vennemann, T.W., Ware, D., Schneebeli-Hermann, E., Hochuli, P.A., Brühwiler, T., Brinkmann, W., Bucher, H., 2012. Climatic and biotic upheavals following the end-Permian mass extinction. Nat. Geosci. 6, 57–60.
Schobben, M., Stebbins, A., Ghaderi, A., Strauss, H., Korn, D., Korte, C., 2015. Flourishing ocean drives the end-Permian marine mass extinction. PNAS 112, 10298–10303.
Scholger, R., Hermann, M.J., Brandner, R., 2000. Permian–Triassic boundary magnetostratigraphy from the Southern Alps (Italy). Earth Planet. Sci. Lett. 176, 495–508.
Schubert, J.K., Bottjer, D.J., 1995. Aftermath of the Permian–Triassic mass extinction event: paleoecology of lower Triassic carbonates in the western USA. Palaeogeogr. Palaeoclimatol. Palaeoecol. 116, 1–39.
Schubert, J.K., Bottjer, D.J., Simms, M.J., 1992. Paleobiology of the oldest known articulate crinoid. Lethaia 25, 97–110.
Shen, S.-Z., Crowley, J.L., Wang, Y., Bowring, S.A., Erwin, D.H., Sadler, P.M., Cao, C.-Q., Rothman, D.H., Henderson, C., Ramezani, J., Zhang, H., Shen, Y., Wang, X.-D., Wang, W., Mu, L., Li, W.-Z., Tang, Y.-G., Liu, X.-L., Liu, L.-J., Zeng, Y., Jiang, Y.-F., Jin, Y.-G., 2011. Calibrating the end-Permian mass extinction. Science 334, 1367–1372.
Šimo, Olšavskỳ, V., 2007. *Diplocraterion parallelum* Torell, 1870, and other trace fossils from the Lower Triassic succession of the Drienok Nappe in the Western Carpathians, Slovakia. Bull. Geosci. 82, 163–173.
Stanley, S.M., 2009. Evidence from ammonoids and conodonts for multiple Early Triassic mass extinctions. Proc. Natl. Acad. Sci. U. S. A. 106, 1564–1567.
Steckbauer, A., Duarte, C.M., Carstensen, J., Vaquer-Sunyer, R., Conley, D.J., 2011. Ecosystem impacts of hypoxia: thresholds of hypoxia and pathways to recovery. Environ. Res. Lett. 6, 1–12.
Sun, Y., Joachimski, M.M., Wignall, P.B., Yan, C., Chen, Y., Jiang, H., Wang, L., Lai, X., 2012. Lethally hot temperatures during the early Triassic greenhouse. Science 338, 366–370.
Twitchett, R.J., 1999. Palaeoenvironments and faunal recovery after the end-Permian mass extinction. Palaeogeogr. Palaeoclimatol. Palaeoecol. 154, 27–37.
Twitchett, R.J., 2006. The palaeoclimatology, palaeoecology and palaeoenvironmental analysis of mass extinction events. Palaeogeogr. Palaeoclimatol. Palaeoecol. 232, 190–213.
Twitchett, R.J., 2007. The Lilliput effect in the aftermath of the end-Permian extinction event. Palaeogeogr. Palaeoclimatol. Palaeoecol. 252, 132–144.
Twitchett, R.J., Barras, C.G., 2004. Trace fossils in the aftermath of mass extinction events. Geol. Soc. Lond., Spec. Publ. 228, 397–418.
Twitchett, R.J., Wignall, P.B., 1996. Trace fossils and the aftermath of the Permo-Triassic mass extinction: evidence from northern Italy. Palaeogeogr. Palaeoclimatol. Palaeoecol. 124, 137–151.
Twitchett, R.J., Krystyn, L., Baud, A., Wheeley, J.R., Richoz, S., 2004. Rapid marine recovery after the end-Permian mass-extinction event in the absence of marine anoxia. Geology 32, 805–808.
Twitchett, R.J., Feinberg, J.M., O'Conner, D.D., Alvarez, W., McCollum, L.B., 2005. Early Triassic ophiuroids: their paleoecology taphonomy, and distribution. Palaios 20, 213–223.
Velledits, F., Péró, C., Blau, J., Senowbari-Daryan, B., Kovács, S., Piros, O., Pocsai, T., Szügyi-Simon, H., Dumitricia, P., Pálfy, J., 2011. The oldest Triassic platform margin reef from the Alpine–Carpathian region (Aggtelek, NE Hungary): platform evolution, reefal biota and biostratiagraphic framework. Riv. Ital. Paleontol. Stratigr. 117, 221–268.
Verschuren, D., Tibby, J., Sabbe, K., Roberts, N., 2000. Effects of depth, salinity and substrate o the invertebrate community of a fluctuating tropical lake. Ecology 81, 164–182.
Webb, A.E., Leighton, L.R., 2011. Exploring the ecological dynamics of extinction. Quantifying the Evolution of Early Life 185, pp. 185–220.
Wignall, P., Hallam, A., 1993. Griesbachian (Earliest Triassic) palaeoenvironmental changes in the Salt Range, Pakistan and southeast China and their bearing on the Permo-Triassic mass extinction. Palaeogeogr. Palaeoclimatol. Palaeoecol. 102, 215–237.
Wignall, P.B., Morante, R., Newton, R., 1998. The Permo-Triassic transition in Spitsbergen: $\delta^{13}C_{org}$ chemostratigraphy, Fe and S geochemistry, facies, fauna and trace fossils. Geol. Mag. 135, 47–62.
Worsley, D., Mørk, A., 2001. The environmental significance of the trace fossil *Rhizocorallium jenense* in the lower Triassic of western Spitsbergen. Polar Res. 20, 37–48.
Yochelson, E.L., 2011. Carboniferous Scaphopoda (Mollusca) and non-scaphopods from Scotland. Scott. J. Geol. 47, 67–79.
Zatoń, M., Taylor, P.D., Vinn, O., 2013. Early Triassic (Spathian) post-extinction microconchids from western Pangea. J. Paleontol. 87, 159–165.
Zonneveld, J.-P., Gingras, M.K., Beatty, T.W., 2010. Diverse ichnofossil assemblages following the PT mass extinction, lower Triassic, Alberta and British Columbia, Canada: evidence for shallow marine refugia on the Northwestern coast of Pangea. Palaios 25, 368–392.